The Dissertation Committee for Thomas James Bushart Certifies that this is the approved version of the following dissertation:

Studies of Ca^{2+}-ATPase Involvement in the Gravity-Directed Calcium Current and Polar Axis Alignment of Germinating *Ceratopteris richardii* Spores

Committee:

Stanley J. Roux, Jr., Supervisor

R. Malcolm Brown, Jr.

Karen S. Browning

Enamul Huq

Alan M. Lloyd

Studies of Ca^{2+}-ATPase Involvement in the Gravity-Directed Calcium Current and Polar Axis Alignment of Germinating *Ceratopteris richardii* Spores

by

Thomas James Bushart, B.S.

Dissertation

Presented to the Faculty of the Graduate School of

The University of Texas at Austin

in Partial Fulfillment

of the Requirements

for the Degree of

Doctor of Philosophy

The University of Texas at Austin

May, 2007

Acknowledgements

Every member of Dr. Stanley Roux's lab since I joined has played a part in my success. Special thanks to Dr. Roux and to my project partners, Dr. Mari Salmi and Dr. Stephen Stout. Thanks as well to Aeraj ul Haque, Dr. Enamul Huq and his lab members, Gwen Gage, and Brian Stockus. Finally, both of my parents deserve much credit for giving me the foundations to succeed.

Studies of Ca^{2+}-ATPase Involvement in the Gravity-Directed Calcium Current and Polar Axis Alignment of Germinating *Ceratopteris richardii* Spores

Publication No._____

Thomas James Bushart, Ph. D.

The University of Texas at Austin, 2007

Supervisor: Stanley J. Roux Jr.

All organisms have been subjected to and have evolved with the ubiquitous force of gravity, and most exhibit the ability to sense and respond to this stimulus. To simplify an investigation of the molecular components of a cell's gravity response, this dissertation employs the single-celled spores of the fern *Ceratopteris richardii*. These spores have a polar calcium flux that is determined by the gravity vector, but an understanding of what the molecular components driving this flux are and how they influence subsequent developmental processes is lacking. Of the possible molecular components, available literature pointed to Ca^{2+}-ATPase transporters as an obvious key participant and so they were selected as the main molecule of investigation.

Our results describe the first cloned Ca^{2+}-ATPase from *C. richardii*, CrACA1. CrACA1 has high similarity to known plant Ca^{2+}-ATPases, specifically plasma membrane (PM) Ca^{2+}-ATPases from *Arabidopsis*, and exhibits *in vivo* Ca^{2+}-ATPase activity. An improved method for the statistical analysis and presentation of qualitative

RT-PCR data was employed. The RNA, as well as the protein, of CrACA1 is present during the polarity fixation window which supported the need for further analyses of the role of Ca^{2+}-ATPases.

Our results showing that Ca^{2+}-ATPase inhibitors significantly alter the gravity-directed calcium flux of spores are consistent with previous work but offer valuable new insights. The spore PM Ca^{2+}-ATPases have large impacts on the calcium flux and rhizoid growth but no appreciable impact on polar axis alignment. The results on endomembrane-type Ca^{2+}-ATPases make it clear that this class of pumps has major roles in both axis alignment and tip growth; rhizoid growth is inhibited but alignment to the gravity vector is improved.

The updated model for gravity perception responses in *C. richardii* spores places a strong emphasis on calcium channels and Ca^{2+}-ATPases working in concert to result in a bottom-localized calcium pool to align the polar axis with hints of store-operated calcium mobilization. The work presented represents an increase in our knowledge of one way a single cell can respond to the force of gravity, offering testable hypotheses to further refine gravity perception models incorporating calcium localization.

Table of Contents

List of Tables

List of Figures

Chapter 1: Introduction

All organisms require the ability to sense and respond to stimuli from their environment. At the most basic level an organism's perception of its environment occurs in individual cells, and, even beyond that, at a molecular level. In order for a stimulus to be perceived, it must interact in some fashion with a molecular receptor of a cell. A sense as varied as smell is simply the recognition of a chemical by a receptor at the surface of a specialized neuronal cell. Even more abstract senses, such as light perception by the eye or by a plant leaf, still function by the capturing of light energy by a pigment which leads to changes in other effectors in a signal transduction pathway, ultimately leading to a response by the cell. Of the myriad signals that any organism may perceive, gravity is one of the least understood in terms of its perception and signal transduction pathway.

GRAVITY AND PLANTS

Gravity is a ubiquitous force that all organisms are subjected to and have evolved with. Many varied organisms use gravity as an environmental cue for orienting their bodies. Even in buoyant aquatic environments the force of gravity is an orienting tool. In order to properly function, most animals require that their bodies be positioned in a specific manner in relation to the gravity vector. For plants, gravity is an important signal in addition to or in the absence of other environmental signals. As an autotroph, a plant needs to maintain contact with sunlight, its energy source. The vast majority of plant types are sedentary, lacking the ability to dramatically alter their locations, and therefore have the need to maintain the orientation of their photosynthetic organs towards the light. Even motile algae need to remain at the surface of the water column to receive adequate light intensities. However, day/night cycles, shading, water depth, and soil cover do not always allow for light itself to be used as an orienting signal. A clear example of this is

the light avoidance of roots. Below a certain depth the light signal is absent, yet roots continue to grow downward. Gravity is an exploitable omnipresent and vectorial force that organisms can use in addition to or in the absence of other cues.

That plants can sense and respond to the gravity vector is easily observable. One need only to turn a terrestrial plant on its side to observe the growth changes gravity can induce, even in the absence of other stimuli. Investigations into the responses and response pathways have enjoyed the most successes, but it still remains unclear as to how plants can sense gravity at a cellular level. The majority of investigations have focused on responses to reorientation.

As mentioned, vascular plants most clearly respond through differential growth of cells in their shoots or roots. Maize shoots respond by accelerated growth on the downward edges of their pulvini, while plants like *Arabidopsis* exhibit their differential growth patterns at their elongation zones. At least in the case of *Arabidopsis* roots, however, the tissues responsible for the morphological changes are not those that sense and interpret the gravity vector. Gravitropic responses can be inhibited by removal of specific cells within the root tip called columella (Blancaflor et al., 1998). Intact roots respond correctly through a signal to the elongation zone, where curvature is mediated through relocation of auxin transport proteins. The asymmetric movement of auxin uptake and efflux proteins within the elongation zone causes relatively more growth on the upper surface of the root, leading to downward curvature until the columella cells are returned to vertical alignment (for a review of gravity induced signal transduction in roots see Perrin et al. (2005).

The auxin redistribution and growth changes in angiosperms are well characterized, but the sensing and transmission signals for the gravity signal are not as clear. However, it is apparent that the sensing mechanism still occurs at the cellular level

even in a multicellular organism. Investigations into motile algae, C*hara*, *Ceratopteris*, and other systems have revealed that single cells of surprisingly small mass are capable of sensing the gravity vector. Since single-celled organisms can sense and respond to gravity as well, it seems likely that there is a shared primitive mechanism by which a single cell is capable of perceiving this particular component of its environment.

Gravitational sensing models

The two favored hypotheses regarding gravity perception by a single cell are the gravitational pressure model and statolith model. While the two models have certain unique features, they are not necessarily mutually exclusive. In general, the gravitational pressure model states that the mass of the cell as a whole causes tension and compression forces on the cell membrane and/or cytoskeleton. The statolith model is more internally focused; organelles, specifically high-density starch-containing ones, move or sediment within the cytoplasm with the vector of gravity. The movement of the organelles is sensed via the cytoskeleton or direct contact with internal or plasma membranes.

In the gravitational pressure model, the mass of the cell's protoplasm causes an uneven pressure distribution around the surface of the cell. The cell then uses this uneven force in order to determine "up," most probably by tension and compression forces acting on its own membrane, ECM, and/or actin cytoskeleton. One consideration of this model is that in order for gravity to have an impact there must be a difference in pressures, and since cells exist in a surrounding environment, one must consider buoyancy. This is perhaps best envisioned by imagining the cell as a balloon filled with water. If you place the balloon on a flat surface it will sag. Since the balloon is denser than the surrounding air it "falls" downward and the bottom of the balloon experiences more pressure than the top due to static equilibrium necessitating a counteractive force of the surface. However, if you were to place that balloon in water instead of air it would take on a more rounded

shape since the pressures inside and outside the balloon have become closer to equal. You could even reverse the first situation by instead filling the balloon with helium and letting it go in a room. It would float towards the ceiling and experience pressure on its top surface, this occurring because the density inside the balloon is now less than the surrounding medium of the air. Translating this back into the system of a living cell, the direction and magnitude of the gravitational vector as experienced by the cell is dependent on its buoyancy in relation to its surrounding media. This is quite useful for testing the model because buoyancy is a much easier parameter to modify than gravity. A number of researchers have done experiments that illustrate this.

Increasing the density of the external media is a simple way in which to effectively decrease the perceived gravitational force on a cell. Doing so can impede the gravity response and even reverse it in *Chara* internodal cells and rice roots (Staves et al., 1997a; 1997b). In the case of *Chara*, the ratio of cytoplasmic streaming seen in vertically-oriented internodal cells becomes "1" at densities equal to the protoplast, while higher densities drop the ratio below that point (normally the cells exhibit a 1.1:1 ratio). In rice plants the downward curvature of their roots becomes lessened at higher external densities while still maintaining normal growth rates. Staves et al. could not replicate the reversal of gravitropic response with rice, which they attribute to difficulty with the higher natural density of the columella cells. The same experiments performed in *Euglena*, a motile protozoan-like alga, show similar results to the *Chara* internodal cells. In the case of *Euglena*, gravity response is measured by taxis away from the gravity vector, movement which becomes random when, as determined by space flight experiments, gravity is less than 0.16 of normal. Directional movement could be impaired without effects on taxis rates, and again even reversed, by increasing media density (Hader and Hemmersbach, 1997). The idea that pressure is the main impact gravity has

on cells is further illustrated by modulating the hydrostatic pressure on *Chara* internodal cells. Application of pressure or vacuum to only one end of a horizontally-positioned internodal cell can cause a response as if the stimulated end were facing downward or upward respectively (Staves et al., 1992).

The premise of the statolith model comes from observations of organelle behavior in positionally altered cells. One of the most studied is the sedimenting of dense starch-containing amyloplasts in the columella cells of *Arabidopsis* roots. These amyloplasts will settle to the new downward direction of the cells when a vertically oriented root is placed horizontally. The importance of the sedimenting statolith can be seen in reduced-starch mutant plants because they exhibit a decreased gravity response in both their hypocotyls and roots (Kiss et al., 1996; Kiss et al., 1997), with a corresponding decrease in plastid sedimentation ability (MacCleery and Kiss, 1999). Additionally, external manipulations of the statoliths can lead to responses similar to being gravistimulated, such as seen with the application of a magnetic field to *Arabidopsis* roots and moss protonema (Kuznetsov and Hasenstein, 1996; Kuznetsov et al., 1999). Wild-type roots responded as expected from amyloplast movement, while a starchless mutant was non-responsive. In moss, both wild type and "wrong way response" mutants responded as predicted by the movement of their plastids within the magnetic field. Laser trapping manipulation of statoliths also causes gravitropically similar responses in *Chara* cells (Braun, 2002). There are indications that specialized membranes may be involved in the transduction of a sedimentation signal. Yoder et al. (2001) identified specialized stacks of endoplasmic reticulum underneath amyloplasts, and Braun (2002) delimited the sensitive areas of plasma membranes. These ER structures would presumably experience compressional forces on their membranes which could be translated into a signaling response through components in the membrane or within the ER lumen.

Neither model is wholly complete enough to explain the gravity perception of every type of cell. The pressure model was inconclusive when tested on moss, a system which does exhibit organelle sedimentation much like rice roots. Alterations of the external media do decrease the responsiveness of the protonema in a density-dependent manner, yet the authors conclude that their data supports the statolith model because of the inability for higher densities to reverse the gravitropic response (Schwuchow et al., 2002). Critics of the *Chara* results also point out that the internodal cells are in the centimeter-size range, making any pressures experienced by such a cell being vertically oriented much greater than that of a typical plant cell. In regards to the statolith model, cells with deficient amyloplasts have reduced, but not wholly absent, gravity responses (Kiss et al., 1996; Kiss et al., 1997). It is also the case that dense particles necessarily increase the density of a cell as a whole (from the previous example, imagine placing marbles in the water balloon). There are also gravity-responsive cell types that do not have dense particles for sedimentation, so the statolith model is not adequate on its own either. As well, the rhizoids and protonema of *Chara* have statolith-based gravity responses, indicating that even within one organism more than one method may be employed. Limbache et al. (2005) have even suggested that statoliths may function through molecular interactions between membranes rather than compression forces. However, either of the models requires a similar end point, interactions with the cytoskeleton and membrane systems. In addition, both acknowledge that gravity must first physically act upon a component of the cell.

CERATOPTERIS AS A GRAVITATIONAL MODEL SYSTEM

As a means of simplifying the investigations of the molecular components of a cell's gravity response, the gametophyte spores of the semi-aquatic fern *Ceratopteris richardii* have been employed. The major benefit of the *C. richardii* spore system is that

the single-celled spores are capable of both sensing and responding to the gravity vector, eliminating the signaling complications of multicellular plants. As well, the spores are responsive within a limited window, allowing us to narrow our focus to a specific time frame. In terms of the gravity perception models, the spores are of a composition and size that lend themselves to elaboration of the gravitational pressure model. They do not appear to require additional internal elements, such as the statoliths of columella cells. The nucleus does migrate downward, but in microgravity conditions the nucleus migrates in a random direction yet is still predictive of future polar events (Roux et al., 2003). As well, the timing of nuclear migration occurs after polarity has been fixed in the spore. The timing of the nuclear movement and its behavior in microgravity indicate that the nuclear movement is a consequence of an established polar axis and not a statolith-like sedimentation. As well, unlike a *Chara* cell, which may be hundreds of thousands of times the size of a columella cell, *C. richardii* spores are only around 100 μM in diameter. While there is an inherent bias for the pressure model due to lack of obvious statolith elements, statolith-containing systems are still capable of pressure-related responses within the same cells or other parts of the same organism. *Ceratopteris* is an ideal system for studying at least one model of how any single cell might both perceive and respond to the gravity vector.

As a general system, *Ceratopteris* has certain advantages. While transformational techniques are still unfortunately quite limited (Rutherford et al., 2004), *C. richardii* does have a manageable generation time of around three months. The sporophyte can make millions of spores and continue producing spore-bearing fronds for many months. The spores and gametophytes, the two growth stages of most interest for my studies, are easy to germinate in the lab under controlled conditions. Spores will remain dormant and viable for many years, until hydrated and exposed to light. Limited maintenance of

hydrated spores in the dark (around one to two weeks) leads to increased synchronicity of germination for the population. Availability of large numbers of synchronous spores makes the gametophyte stage very useful for both statistical analysis of responses and examination of molecular elements such as RNA and protein levels. Specific to gravity-related studies, *C. richardii* spores are ideal due to several quantifiable gravity-directed responses that occur within a limited window of sensitivity.

The germinating spores of *C. richardii* proceed through a number of developmental steps that are influenced by the gravity vector. After the initiation of germination, the nucleus migrates, an asymmetric cell division occurs, and the primary rhizoid emerges. The direction of nuclear migration and rhizoid growth follows the gravity vector and the cell division occurs in a plane perpendicular to it. The commitment of the spore to this polar growth is established within the first 24 hours after initiation of germination. Reorientation of the spore after 24 hours will result in rhizoid growth in the direction that was originally downward (Edwards and Roux, 1998). This means we can focus our investigations on processes occurring in the spore prior to 24 hours after light exposure.

Of particular interest to my own research is a calcium flux that occurs before the spore is committed to its growth direction. Using a self-referencing ion selective probe, the flux of calcium ions was measured at various points around the spore. An efflux of calcium was found to occur at the top of the spore, while there was an accompanying influx at the bottom of the spore (Chatterjee et al., 2000). The directionality of the flux corresponds to the gravity vector since after turning the spores 180°, the calcium flux also turns 180° to reorient. This reorientation occurs quite rapidly. Using the same probe, Stout (2004) showed that the direction of the polarized calcium flux was reversed faster than 42 seconds after rotation. The use of a new sensor set up that allows for continuous

measurements even during reorientation has shown that the calcium flux response aligns to the gravity vector within about 24 seconds (Salmi et al., 2007). Having a fast-reacting, molecularly driven, and measurable response to the gravity vector, coupled with ease of handling makes *C. richardii* spores an ideal system for getting closer to the roots of a single cell's gravity perception mechanisms.

Clarification of terms of polarity

There are a number of terms to consider when discussing development in relation to a directional signal. Using the guidelines established by Cove (2000), we can consider three aspects of polarity in relation to the *C. richardii* spore system. First, the spores exhibit axis polarity in that rhizoids and thalli grow in roughly opposite directions. Second, the spores exhibit axis alignment, whereby the polar growth of the rhizoid is aligned with the vector of gravity. Finally, the germinating spores also have an axis orientation; the rhizoid specifically grows in the same direction as the vector of gravity. The alignment of the spores, namely the percentage of spores that exhibit downward rhizoid growth, is a condition that can change in a significant manner. This should not be confused with orientation. Changes in orientation have been characterized, such as when unilateral light is shown at an angle perpendicular to the gravity vector. In that case the rhizoid orientation shifted to fall at a point between directly downward and directly away from the light (Edwards and Roux, 1998). However, the treatments presented here only appear to show an increase or decrease in the number of downward growing rhizoids, i.e. changes in alignment. It is notable that *C. richardii* spores appear to be capable of establishing their polar axis in the absence of a strong external signal. Spores grown in the microgravity environment of a space flight still develop and produce rhizoids, but the growth direction is random (Roux et al., 2003). Presumably this is because the signal for

orientation (gravity) is not strong enough and so alignment occurs randomly or arbitrarily.

GRAVITY RESPONSES AND CALCIUM

The application of nifedipine, a calcium channel blocker, decreases the gravity-directed Ca^{2+} efflux forty fold, and subsequent downward rhizoid emergence is disrupted (Chatterjee et al., 2000). Nifedipine abolishes the gravity response in *Chara* internodal cells as well (Wayne et al., 1992). This suggests that movement of calcium is necessary for gravity-directed development, and is especially interesting since it is thus far the earliest observable response.

While the calcium flux is influenced by the gravity vector, it remains to be firmly established how these changes in Ca^{2+} ion concentrations affect subsequent developmental processes. Comparison of the *C. richardii* calcium flux to other known developmental ion movements suggests that it may have a unique function. Fertilization in plants is accompanied by an influx of calcium ions, but the influx is homogenous over the entire cell (Antoine et al., 2000). Growth is accompanied by calcium movement as well. *Fucus* cells show a concentration of Ca^{2+} localized to the growing rhizoid, and pollen tubes show a similar calcium distribution at their growing tips (Brownlee and Pulsford, 1988) (see also the introduction to Chapter 3). In these cases, however, calcium seems more associated with new membrane growth. Since the *C. richardii* calcium flux occurs hours before the first cell division, and days before the rhizoid emerges, it is unlikely that this flux is directly growth associated. Rather, the timing of the flux correlates to the gravity-directed polarity fixation window, and more specifically to the random movement of the nucleus at the center of the cell, ending roughly when the nucleus commits to downward migration (Edwards and Roux, 1998). The difference in composition of the flux is also of note. Fertilization-based polarization in the order

Fucales is accompanied by a proton gradient while there is no similar H^+ movement in the early germination of *C. richardii* spores (Chatterjee et al., 2000). Again, this indicates that the observed calcium flux is involved in a different process and the proteins involved warrant investigation.

Since a resting cell maintains extremely low concentrations of calcium in its cytoplasm, the electrochemical gradient favors the movement of calcium into the cytoplasm. This is of benefit to rapid calcium signaling because dramatic changes in cytoplasmic calcium can be achieved through very little energy input. In connection to the calcium flux then, the influx of calcium into the bottom of the spore is most likely through passive transport, such as that of a calcium channel. As mentioned above, calcium channel blockers both inhibit the flux and disorient the spore's alignment to the gravity vector. Thus it is likely that the major component of the bottom-side calcium flux is a calcium channel. However, the study of calcium channels is problematic in plant systems. At the start of my project there was limited information regarding calcium channels in plants, specifically a lack of identified genes. Even with the sequencing of the *Arabidopsis* genome, no clearly identifiable genes for channels are known. The vast majority of calcium channel characterizations involved patch clamping to analyze the behavior of membranes under various conditions. This technique supplied a good deal of characterization and classification of membrane responses but is not particularly useful for manipulations, especially in our system where it is difficult to get direct access to the membrane due to the spore coat. The involvement of calcium channels is considered and discussed, but no direct assays of them are done in this presented work.

The other component of the calcium flux is the topside outward movement. This efflux of calcium is of a much greater magnitude than the influx at the bottom, suggesting a potentially greater role in gravity-directed alignment. Since this direction of calcium

movement is against the electrochemical gradient, the process would require energy input for active transport. Of the possible molecular candidates for this, Ca^{2+}-ATPases are the most attractive based on several factors. First, they are active transporters, fulfilling the energy-dependent requirement. Second, certain subclasses localize to the plasma membrane, the location necessary for being the main player in an outwardly directed calcium movement. Third, their activity is subject to regulation through calmodulin and phosphorylation (Rasi-Caldogno et al., 1995; Evans and Williams, 1998; Bonza et al., 2000; Chung et al., 2000; Geisler et al., 2000), a feature likely necessary for a polar response limited to a specific time frame and location. Last, there exists ample sequence information and characterization of Ca^{2+}-ATPases from plant and animal systems to make meaningful comparisons. For these reasons, Ca^{2+}-ATPases were selected as the main molecule of investigation to connect the observable gravity-directed calcium current to gravity-directed polarity.

SUMMARY

Gravity is a ubiquitous and useful force for organisms to orient themselves. The mechanisms behind gravity sensing and early transduction pathways of single cells have yet to be fully elucidated. To that end, the model system of *C. richardii* spores and gametophytes have been employed.

C. richardii spores have several factors that make them attractive as a model system for gravity-based research. Beyond superficial qualities such as synchronous growth and ease of handling, the alignment of the spores' axis of polarity is limited to a window of sensitivity between 0 and 24 hours post light exposure, allowing for a focused investigation. Polarity alignment can be measured visually at the stages of nucleus migration or rhizoid emergence, or is can be measured molecularly even earlier, during the fixation window, through a polar calcium flux.

The responsiveness of the calcium flux to the gravity vector, combined with its presence during the polarity fixation window, makes it one of the best candidates for studying the connection of early gravity-directed molecular events to subsequent axis establishment/alignment. Due to the lack of readily identifiable calcium channels in plant systems, the involvement of Ca^{2+}-ATPases have been investigated. Due to their various properties, Ca^{2+}-ATPases are the most probable component of the calcium efflux.

The work presented here examines the sequence similarities of the first cloned *C. richardii* Ca^{2+}-ATPase (CrACA1) to other known plant Ca^{2+}-ATPases to make comparisons in function. The RNA expression profile of CrACA1 during the window of polarity fixation was examined using real-time RT-PCR techniques. The protein expression was determined over the same time frame to compare RNA and protein presence. Finally, the connection between the spores' calcium flux and axis alignment was determined using Ca^{2+}-ATPase inhibitors and a newly designed measurement system. Taken together, this dissertation presents the characterization of a new Ca^{2+}-ATPase and the involvement of Ca^{2+} and Ca^{2+} pumps in polarity establishment and polar growth.

Chapter 2: Cloning and Profiling of a Ca^{2+}-ATPase from Germinating Spores

INTRODUCTION

Rationale

The control of calcium levels in living cells is important for signaling and homeostasis. Among the numerous processes that calcium is involved in, tip growth and the establishment of polarity in single cells are the most relevant to the research described in this chapter. Both of these processes depend on the movement of calcium across membranes, and thus the activity of calcium transport proteins, in order to alter concentrations and localizations. There are a limited number of classes of calcium transporters in plant cells, falling into the categories of calcium channels, cation/H^+ exchangers (CAX), and calcium ATPases.

Calcium channels are believed to play a very important role in many cellular processes, including that of gravity sensing (Chatterjee et al., 2000). However, the majority of analyses of these channels in plants have been limited to patch clamping techniques and general pharmacological treatments due to the lack of identifiable genes encoding these channels. The lack of gene information limits our ability to effectively examine the role of channels in the *Ceratopteris richardii* gravity responses, although in Chapter 3 we gain insights on the importance of these channels through pharmacological modulation of nifedipine-sensitive calcium channels in spores.

The CAX class of calcium transporters appears to have the strongest roles in calcium homeostasis (Moller et al., 1996). Ca^{2+}/H^+ exchangers function largely within the endomembrane systems, most often within the tonoplast of the vacuole, although plasma membrane localization is possible. Their activity is influenced by pH (Pittman et al.,

2005) and their exchange process has been described as similar to the spending of a proton "currency" (Hirschi, 2001; Gaxiola et al., 2002). In plant cells the largest stores of this proton currency are in the vacuole, and the anti-porting activity would favor the movement of Ca^{2+} into the vacuole. The lack of a notable proton gradient associated with the calcium efflux from the top of the spore (Chatterjee et al., 2000) and the typical function and localizations for the CAX class of transporters makes it unlikely that these components would be direct contributors to the calcium efflux.

This leaves the Ca^{2+}-ATPases as the logical choice for investigations related to gravity perception/response, and this choice is further favored by there being both ample and identifiable sequence information and established analyses of activity of these transporters (Geisler et al., 2000). As seen by Chatterjee et al. (2000), the efflux of calcium from the top of the spore is dramatically stronger than the influx occurring at the bottom. Due to the standard homeostasis of cells, calcium is maintained at very low concentrations in the cytoplasm, therefore this efflux is occurring against a concentration gradient. Energy-dependent removal of calcium from the cytoplasm utilizes Ca^{2+}-ATPases both on the plasma membrane for removal from the cell, and on endomembranes for sequestration into internal stores such as the endoplasmic reticulum or vacuoles. Involvement of calcium transport in the polarity establishment of *Ceratopteris* spores is indicated by the inhibition of calcium channels through application of nifedipine, which causes a dramatic reduction in efflux and lowers subsequent proper gravity-directed orientation (Chatterjee et al., 2000). Due to the active transport requirement of calcium efflux and data linking Ca^{2+}-ATPases to gravity-directed polarity, the identification of Ca^{2+}-ATPases in *C. richardii* spores was undertaken.

Plant Ca^{2+}-ATPases

Ca^{2+}-ATPases have been implicated in general calcium homeostasis and stress adaptation as well as specific mechanisms including responses to abscicic acid (Beffagna et al., 2000), pollen tube growth and fertilization (Schiott et al., 2004), and root gravitropism (Urbina et al., 2006). Ion transporting Ca^{2+}-ATPases belong to the general family of P-type ATPases, which are capable of translocating a variety of cations across cellular membranes. A series of extensive reviews published in *Biochimica et Biophysica Acta* cover many of the basic details of P-type ATPases in general (Moller et al., 1996), P-type ATPases in plants (Evans and Williams, 1998), and finally the P-type Ca^{2+}-ATPases of plants (Geisler et al., 2000). Since this study is concerned with the active transport of Ca^{2+} across membranes of *C. richardii* spores, only the features pertinent to plant P-type Ca^{2+}-ATPases will be discussed in detail. Unless otherwise noted the information is from the three specified reviews.

P-type ATPases are primitive and widespread, occurring in both prokaryotic and eukaryotic organisms and are so called due to the formation of a phospho-aspartate intermediate during their enzymatic process. As their name also implies, P-type ATPases use the energy of ATP hydrolysis to drive the movement of ions across membranes. The movement of Ca^{2+} via Ca^{2+}-ATPases is accompanied by a counter movement of protons, but pH does not function in the same regulatory manner as in the CAX transporters. The type II subclass of pumps is capable of moving low atomic mass ions, including Ca^{2+}. The plant Ca^{2+}-ATPases characterized fall into a further subgrouping of type IIA or type IIB. The general characterizations of each type indicate that type IIA pumps are endomembrane (often referred to as SERCA type for sarco(endo)plasmic reticulum Ca^{2+}-ATPases, although obviously only the endoplasmic reticulum designation is relevant for plant cells) while type IIB include a further division of *Arabidopsis thaliana* Ca^{2+}-

ATPases ACA8, 9, and 10. AtACA8 and 9 have been characterized as plasma membrane associated (Bonza et al., 2000; Schiott et al., 2004) and due to the sequence similarity AtACA10 is assumed to be as well.

Type IIB Ca^{2+}-ATPases have an autoinhibitory region that functions as part of its regulation (Rasi-Caldogno et al., 1995). This region has a calmodulin (CaM) binding domain. CaM binding is stimulatory to the Ca^{2+}-ATPase activity by blocking the interaction of the inhibitor region with the rest of the molecule. Phosphorylation can also decrease the autoinhibitory activity. Proteolytic cleavage of the autoinhibitory region results in constitutive activation, and exogenous expression of type IIB Ca^{2+}-ATPases in yeast requires truncated versions lacking this inhibitory region (Harper et al., 1998; Bonza et al., 2000; Chung et al., 2000; Schiott et al., 2004).

Gene expression at the RNA level using real-time RT-PCR[1]

Assays of transcript abundance are often performed in a qualitative manner, simply involving endpoint RT-PCR or Northern blotting to detect RNA levels. Actual quantification of expression levels from these methods is difficult at best, but we now have access to quantitative methods through the procedure of real-time RT-PCR (also called quantitative or qPCR). While qPCR has many advantages over standard end-point PCR or hybridization analyses, it also has a number of technical challenges that make it more complicated, and there are a large number of methods by which RNA levels can be monitored in real time.

qPCR allows for the quantification of the absolute or relative level of any gene transcript of interest. Because of its specificity and sensitivity, it can be used to successfully determine levels of expression for transcripts with very high or extremely low message abundance (reviewed by Gachon et al. (2004)). It has been effectively used

[1] Portions of this section are my own work taken from Salmi et al. (2006).

as a tool to accurately determine message levels for a variety of members of conserved plant gene families. This technique has enabled researchers to study and successfully analyze the expression of several enzyme gene families (Yokoyama and Nishitani, 2001; Tan et al., 2003; Yokoyama et al., 2004). Quantitative real-time RT-PCR is also well suited for expression profiling of signal transduction gene families and can be effectively used to determine expression changes in response to abiotic stresses (Charrier et al., 2002; Adams-Phillips et al., 2004; Jang et al., 2004; Cantero et al., 2006).

qPCR detection methods

There are various types of quantitative real-time RT-PCR but all are based on detection of PCR product as it is being amplified via increased fluorescence (Figure 2.1). The increase in signal follows a typical S-curve, with the region of importance being the exponential phase. The number of cycles it takes to reach the point of exponential increase in signal is dependent upon the amount of starting template for the PCR reaction; lower template concentrations will take longer (more cycles) to achieve the same signal level as compared to higher template concentrations. Since there are a variety of fluorescent tags available, it is possible to detect more than one amplification product in the same tube. Multiplexing requires that each product be labeled differently and monitored at the same time. Multiplex reactions have the advantage of each product experiencing identical amplification conditions, but this aspect is complicated by competitive amplification between products. It may be simpler to carefully control for variations between reactions than trying to optimize a multiplex reaction. Changes in the fluorescent signal are also useful for determining specificity of the reactions through analysis of a melting curve. As the temperature in an end-point PCR reaction increases, the fluorescent probes will undergo transition between high and low signals as their configuration changes. The specifics of this transition depend on the particular assay

system used, as detailed below. Since annealing/dissociation temperatures are based on sequence, each detectable product should give only one signal peak.

The main difference between various methods of RT-PCR is in the detection of the product. Presence of PCR products can be detected through double stranded DNA (dsDNA) binding chemicals, hybridization probes, or hydrolysis probes. At the simplest, a dsDNA binding chemical indicates the addition of product since the starting cDNA template is single stranded (Figure 2.1A). SYBR® Green (Molecular Probes, Invitrogen Corp., Carlsbad, California) is typically used in these instances. This method has the drawback of being very unspecific. Any extraneous PCR products produced in this case will increase the signal, leading to artificially high template concentration calculations. Methods employing dsDNA binding chemicals must be controlled very carefully to avoid this complication. For the same reason, multiplexing is not possible with dsDNA binders. Other methods are more specific, though they vary in terms of costs and ease of use.

Of the remaining two methods, hybridization probes are the more straightforward. Use of hybridizing probes increases the specificity of the measurements since increases in fluorescent signal will only occur in the presence of matching target sequences. These methods typically rely on the use of the Fluorescence Resonance Energy Transfer (FRET) principle to distinguish between free and hybridized probes. In the case of the LightCycler® (Roche, Basel, Switzerland), two neighboring probes are labeled with fluorochromes that have FRET interactions. Successful hybridization by both probes allows for excitation of one fluorochrome and emission detection of the second (Figure 2.1B). In a similar way, molecular beacons (The Public Health Research Institute, Newark, New Jersey) use a quenching moiety to decrease the signal from the unhybridized probe. Here FRET is used to lower the signal in an unbound probe, typically a hairpin structure brings the two elements in close proximity. Signal is detected

at each round of hybridization in the PCR cycle by the increase in fluorescence, when the probe is bound to the target product FRET no longer occurs (Figure 2.1C).

Invitrogen Corp. (Carlsbad, California) uses a Light Upon eXtention (LUX™) method to detect successfully amplified products in a manner similar to molecular beacons. In lieu of FRET and the quencher, however, one of the primers used for PCR is specially designed to have a terminal hairpin structure. The hairpin itself quenches the fluorescent signal such that detection of the product is measured by the increase of signal occurring from incorporation of the primer into a PCR product (Figure 2.1D).

Scorpions® (Molecular Probes, Invitrogen Corp., Carlsbad, California) are another detection mechanism with elements similar to both molecular beacons and the LUX™ system. The structure of the Scorpion® probe has a primer region and a separate hairpin portion. The hairpin region is responsible for FRET quenching of the fluorochrome through proximity of a quencher. The literal twist to this process comes after incorporation of the primer into the product. The loop region of the quenching hairpin has matching sequence to the downstream amplified product. Through an intramolecular binding event, the loop causes the 5' fluorochrome to be moved away from the quencher, giving fluorescent signal. The binding of the 5' end of the Scorpion® primer to the same strand of the product appears much like a scorpion's arched tail, hence the choice of name (Figure 2.1E).

The final variation of real-time RT-PCR product detection uses cleavage of the probe as an indicator of successful amplification. In the case of TaqMan® probes (Applied Biosystems, Foster City, California), FRET quenches the signal from the fluorochrome at the 5' end of the probe. Signal is measured through the release of this fluorochrome via the 5' exonuclease activity of the polymerase as it approaches the

hybridized probe (Figure 2.1F). Signal in these instances is not dependent upon temperatures and annealing of the probe after its initial cleavage.

Choosing a method for detection depends largely on resources and time. SYBR Green® is a cheaper option, and looking at additional genes is as simple as obtaining standard primers, but the method requires careful use and analysis due to its non-specific nature. LUX™ primers and Scorpions® have the benefit of requiring fewer components in the PCR reaction since the indicator becomes incorporated into the product but the detection is unique to each target. Specificity is excellent for molecular beacons and TaqMan® probes, but such experiments can be very costly and may also have difficult end-point analysis. TaqMan® probes, for example, require addition of SYBR Green® for melting curve analyses since fluorescence in this case becomes uncoupled from the actual products. When selecting a detection method, researchers should take into account the required sensitivity, time available, and monetary resources.

For the purposes of studying the Ca^{2+}-ATPases of *C. richardii* the LUX™ system was selected as a middle ground in terms of cost and specificity. Since a large number of genes were not going to be analyzed, the investment in specific primers for CrACA1 and a few control genes was not large. The LUX™ primers are also available with different fluorochromes, allowing for duplex reactions.

qPCR data analysis

Regardless of the detection method used, analysis of the data involves conversion of signal into meaningful measurements of starting template. The two major methods for template calculations are the standard curve method or the comparative C_T method. For the first method, a series of measurements are made on known amounts of starting material in order to construct a standard curve reference for unknown measurement comparison. The standard curve method has the benefit of being useable for determining

template copy numbers. Its main drawback is that the construction of the curve must be very accurate, which may be problematic when dealing with RNA samples. Standardization to an internal control, such as a housekeeping gene, may be required as well. The alternative, the comparative C_T method, does not give absolute copy numbers, but rather gives information regarding relative changes in gene expression. For this method, a control or reference gene is compared to the gene of interest between two conditions, typically treated vs. untreated or different time points. The comparative C_T method requires that the gene of interest be amplified at a similar efficiency level to that of the control gene but requires no additional reactions once efficiency has been established.

Care must be taken with selection of control genes in either case. It is necessary that the genes selected are not significantly altered in expression level in the situations being investigated. This may necessitate some additional work in novel experiments. It is also becoming more advisable to use several control genes for better confidence in outcomes. In a recent study a number of good candidates in *Arabidopsis* were determined (Czechowski et al., 2005). The increasing amounts of publicly available microarray data are invaluable for control gene selection for atypical treatments or conditions. At the time of initial experimentation, the *C. richardii* microarray on the first 5,000 ESTs was not completed so four genes were selected based on common use in other systems and additional work was done with them to determine their usefulness as references.

In Cantero et al. (2006), Sharmistha Barthakur established the gene efficiencies and so data analysis could proceed using the comparative C_T method. However, presentation of data as outlined by the qPCR thermocycler manufacturer (Applied Biosystems, 2004) does not include any method for determining significance of the results. Like many new techniques, qPCR data is too often presented with little

commentary on the significance of expression changes. Similar to microarray, one solution is to just make an arbitrary cut off point in terms of the fold-change in expression levels, with the assumption that changes in RNA levels smaller than the cut off may not be of biological significance. Presumably the most significant genes will have the most significant changes in expression levels. While this is of some use when dealing with large number of genes and a large number of conditions, it is somewhat short-sighted and inappropriately ignores the fine tuning processes that cells may undergo. In addition, when intensively investigating just one or two genes of interest, a pattern of consistent gene expression may exist on a scale smaller than an arbitrary cut off. To that end, I sought to apply statistical methods to the examination of qPCR data, similar to how microarray data published in our lab has been treated (Salmi et al., 2005).

One possibility was the publicly available Excel-based REST© (Relative Expression Software Tool) program that analyzes significance of data through a randomization test (Pfaffl et al., 2002). One limitation with my own data is that this program does not take into consideration different groupings of data. My data was collected over several experiments, which are internally consistent for calculations of delta C_T values. The REST program cannot distinguish between data sets like that, so it was used as a general verification of result trends, but could not give particularly accurate specifics. Instead, I opted to apply a formula for calculation of confidence intervals. Confidence intervals have the advantage of taking into consideration the number of replicas used. As well, they translate into graphical representation, making it possible to tell at a glance which points of data are significantly different from one another.

Experimental goal

Germinating spores exhibit a strong top-side calcium flux during the period of polarity fixation. Based on the characteristics and available information regarding

calcium movement proteins in plants, I undertook the task of identifying the full length sequence of a Ca^{2+}-ATPase present during early spore germination. The cloning, sequence characterization, and expression profiling of this Ca^{2+}-ATPase, designated CrACA1, was performed in order to make further connections between the calcium efflux and polarity fixation.

MATERIALS AND METHODS

Plant materials and growth conditions

Spores from the Hn-n strain of *C. richardii* were surface sterilized and handled as per the literature for eventual RNA isolations (Edwards and Roux, 1998; Salmi et al., 2005). Adult sporophyte plants were grown in soil in the same incubator used for spore germination. Increased humidity for ideal growth of the adult plants was achieved via use of clear plastic dome covers.

Yeast growth conditions

Yeast media used was Yeast Nitrogenous Base (YNB) supplemented with amino acid drop out media as appropriate. YNB without amino acids, yeast synthetic drop-out medium supplement without uracil, and D-(+)-raffinose pentahydrate, glucose, and -galactose were all ordered from Sigma (Sigma-Aldrich, Inc, St. Louis, MO). Liquid media was made by autoclaving the pH adjusted YNB plus amino acids separately and then adding filter-sterilized sugar (2% glucose, 2% galactose, 2% raffinose, or 2% galactose + 1% raffinose). For plates, 2% agar was added included. EGTA was added to a final concentration of 10 mM as needed. All media was brought to a pH of 6.0, a step especially important for those media containing EGTA.

Cloning and subcloning of *CrACA1*

Translated query BLAST searches (blastx) were performed on the initial batch of EST sequences from the 20 hr spore cDNA library, resulting in one positive match to any known Ca^{2+}-ATPases. A variety of methods were employed to obtain additional sequence information from EST Cri2_7_N15_SP6 (Accession BE643069), including cDNA library screening and 5' RACE, but were unsuccessful. The full sequence of CrACA1 was finally obtained through utilization of a modified chromosome walking approach employed by Stout (2004). Briefly, genomic DNA (gDNA) was isolated from adult sporophyte plants using a DNeasy® Plant Mini Kit (Qiagen; Valencia, CA) and digested with Not I, Sac I, and Xho I restriction enzymes. Digested gDNA was ligated with similarly digested pCR2.1 TOPO vector. PCR was performed using a custom made plasmid-specific primer coupled with a gene specific primer designed to be close to the 5' end of the known sequence. Nested PCR was performed with M13 forward or reverse primer as appropriate and a further 5' gene-specific primer to obtain stronger and cleaner bands. The largest and cleanest looking bands were excised and gel-purified for subsequent direct sequencing reactions at the ICMB DNA Core Facility (The University of Texas at Austin). PCR program for both rounds of nested PCR was: 94°C for 3 min.; 35 cycles of 94°C for 30 s, 56°C for 30 s, 72°C for 1 min; 72°C for 10 min. Sequence information obtained from each round was used to design new gene-specific and gene-specific nested primer sets for further sequencing until the theoretical 5' end was reached, at which point a GeneRacer™ (Invitrogen; Carlsbad, CA) kit was used for 5' RACE to capture the final sequence information. The full-length sequence was amplified from cDNA using the Expand High Fidelity PCR System (Roche; Indianapolis, IN), TOPO cloned, and transformed into *E. coli* for long term maintenance in freezer stocks. The Expand PCR program was: 94°C for 2 min.; 10 cycles of 94°C for 15 s, 55°C for 30 s,

72°C for 2 min; 15 cycles of 94°C for 15 s, 55°C for 30 s, 72°C for 2 min + 10 s per cycle; 72°C for 7 min.

The full-length sequence was assembled from the compiled sequence fragments with the aid of the Gene Runner v. 3.05 software (Hastings Software, Inc.). Frame shifts and nonsense codons in the reading frame were corrected by additional rounds of sequencing of the TOPO clone and assembly based on the majority consensus sequence. The final sequence was submitted to GenBank (accession number AY333123).

For the yeast activity assay, several sets of primers were designed for amplification of the full length sequence and an 81 amino acid N-terminal deletion (NTD) sequence of CrACA1. Numerous attempts to sub-clone both forms of CrACA1 into the pYES2 expression vector were unsuccessful using all designed primers and both the TOPO template and cDNA. Sequence information, the TOPO clone, and cDNA were sent to Commonwealth Biotechnologies, Inc. (Richmond, VA) for subcloning of the NTD only. Their initial cloning attempts were unsuccessful but sequencing revealed that the TOPO clone had a 71 base truncation at the 3' end, revealing at least one of the problems with previous sub-cloning attempts. CBI performed further amplification attempts using cDNA but only managed to obtain separate 5' and 3' end products with overlapping middle sequences before determining that this project was beyond their ability to perform. All CBI designed primers were shipped to me along with a record of experiments performed.

I duplicated amplification of the overlapping 5' and 3' end fragments using the Expand system and PCR program as listed above but, as with CBI's attempts, the entire NTD product could not be amplified directly. PCR reactions from the 5' and 3' amplifications were diluted 1:10 and 5 µL of each used as template for PCR amplification using the Expand system with a modified program using 2-step

amplification in the second stage: 94°C for 2 min.; 10 cycles of 94°C for 15 s, 60°C for 30 s, 72°C for 2 min; 15 cycles of 94°C for 10 s, 70°C for 2 min + 10 s per cycle; 72°C for 10 min. The prominent band that ran at around 3,000 bp was excised and gel purified for use as template in another round of PCR using the same primers and conditions to produce more product for TOPO cloning. Likely clones were sent for sequencing at the ICMB DNA Core Facility and the desired insert was verified.

The TOPO vector containing the NTD insert was digested with Bam HI and Xho I and ligated into a similarly treated pYES2 vector and transformed into *E. coli*. After sequence verification, DNA designated as pYES2·NTD was prepared by mini preps of overnight cultures for use in yeast transformations.

Confirmation of individual yeast transformants was performed by PCR on crude yeast extracts before use in growth assays. Individual, large yeast colonies of potential transformants were scrapped from the plates and vortexed in 500 µL of sterile water. The suspended yeast were streaked out on labeled plates and the remainder of the solution boiled for 10 minutes. 15 µL of boiled yeast was sufficient template for PCR using the BUSH F5 and BUSH R3 primer set (~770 bp product). Colonies confirmed as positive transformants were used for the growth assay.

The original CBI-designed forward primer lacked a Kozak initiation site. PCR was performed using the Expand enzyme and the above 2-step amplification process using a slightly more 3' primer containing a Kozak start sequence and Bam HI restriction site with the initial pYES2·NTD as template. The resulting PCR product was isolated and treated as above resulting in a second construct designated as pYES2·NTD2.

Sequence Analysis

The full-length nucleotide sequence was compared to other sequences using the NCBI translated query (blastx) program. Those matches having an expect value of 0.0

and definitive gene identities were selected for sequence alignments using a web-based Clustal W alignment program (Labarga et al., 2005; Pillai et al., 2005). Annotation of the CrACA1 protein sequence was done based on alignments to *Arabidopsis thaliana* Ca-ATPases' known structures.

RNA Isolation and cDNA Preparation

Spore samples were collected as a time course of light exposure by freezing one plate every 3 hours starting from the time of light exposure (designated 0 h). Total RNA was isolated and handled from the frozen samples as described in Salmi et al. (2005). 1 μg of total RNA was treated with DNase I and was reverse transcribed using SuperScript® II Reverse Transcriptase (Invitrogen; Carlsbad, CA) with oligo$(dT)_{22}$ primer per the manufacturers recommendations using a thermocycler for incubations.

Real-time RT-PCR

LUX™-based real-time RT-PCR was selected for its balance of sensitivity and cost. Primers were designed using Invitrogen's web-based primer design software. Four different potential control genes, α-tubulin (BQ086953), APT1 (BE640734), actin, and ubiquitin, were selected based on their use as controls in other systems. Primers were ordered for the control genes and the gene of interest, CrACA1 (AY333123). Subsequent evaluations of the designed primers after additional EST sequencing revealed that ubiquitin and actin would be unsuitable due to possible amplification of other gene family members. APT1 and α-tubulin have been demonstrated to function equivalently as reference genes and used in published work (Salmi et al., 2005). They also lack significant expression changes over early time points based on microarray analysis and have minimal sequence similarity to other Ceratopteris ESTs. APT1 was chosen for the control gene for all experiments presented here. Consistent with other primer sets

designed, control gene primers were labeled with the fluorochrome JOE, while CrACA1 primers were labeled with FAM

Initial real-time RT-PCR reactions were carried out as duplexes, each reaction containing the primers for APT1 and CrACA1. Duplex PCR reactions were found to be wholly unacceptable due to extreme variance and non-reproducibility so singleplex reactions were employed instead. Variability from running the APT1 and CrACA1 reactions in separate wells was minimized by use of commercial enzyme preparations, large volumes of master mix, and repetition of reactions in at least triplicate. This method was found to be easily reproducible and gave high quality data.

Reactions were run on a 7900HT Sequence Detector machine (Applied Biosystems; Foster City, CA) as an absolute quantification run. PCR reactions were performed in 96-well polypropylene microplates using Platinum® Quantitative PCR SuperMix-UDG polymerase master mix (Invitrogen) at one-half final volumes (25 µL) according to the Invitrogen cycling programs and protocols. A final concentration of 50 nM of appropriate gene-specific primers and the equivalent of 100 ng of reverse-transcribed RNA were used per reaction. Reaction conditions used were: 50°C for 2 min.;95°C for 2 min.;40 or 45 cycles of 95°C for 15 s, 55°C for 30 s, 72°C for 30 s, followed by the software's default melting curve analysis.

My previously established guidelines require a minimum of six useable data points, taken from at least two technical replicates of three biological replicates (Cantero et al., 2006). Final data was calculated from reactions run in triplicate from three separate RNA isolations performed on different days, yielding up to nine data points for each time point. The actual *n* value range for each time point was eight or nine. Standard curves were generated from five-fold serial dilutions of cDNA pooled from all time points.

Concentrations of the standard curve were arbitrarily assigned based on the lowest concentration being "1."

Data analysis

Initial analysis of presented data was done using the SDS v.2.2.1 software (Applied Biosystems; Foster City, CA). Amplification curves were examined for quality and reproducibility within replicates. Single target amplification of all samples and absence of genomic DNA in mock RT controls was verified via dissociation curve analysis. Data points showing multiple or shifted peaks under the melting curve analysis, as well as those exhibiting irregular amplification curves, were excluded from further analysis. Baselines and thresholds were set manually based on amplification plots, with typical baselines running from cycles 3 through 15 and threshold values selected within the early exponential portion of the plot. C_T values were exported for expression calculations using Microsoft Office Excel 2003 (Microsoft Corporation; Redmond, WA).

The amplification efficiencies for APT1 and CrACA1 were not similar enough to use the comparative ("ΔC_T") method used previously (Cantero et al., 2006). Rather than attempt to design primers and modify reaction conditions to bring the efficiencies in line, data analysis was done using the standard curve method as described in Applied Biosystem's relative quantitation guide (Applied Biosystems, 2004) in the following way. Standard curves were made by plotting the ln([RNA]) vs. C_T values. The formula describing the best fit line was calculated and applied to experimentally determined C_T values to calculate a relative [RNA]. Average C_T values and their standard deviations were calculated for technical replicates. Normalized averages for the biological replicates were calculated by dividing average CrACA1 values by APT values, standard deviations for these normalized figures were calculated using the coefficient of variation. Fold changes in [RNA] over the time course were determined by dividing by the reference

time point of 0h (which sets that time point to a value of "1"). Finally, a single normalized average and standard deviation was calculated from these three normalized fold changes of the biological replicates. To improve on the data calculations I performed in Salmi et al. (2005), 95% confidence intervals of the fold changes were calculated from the average, standard deviation, and *n* values of these final numbers using the using the two-tailed distribution formula similar to the one I used in (Cantero et al., 2006):

$$\overline{X} \pm t_{\alpha(n-1)} \frac{s}{\sqrt{n}}$$

When fold changes are calculated from ratios (as presented here) the 95% confidence intervals are of equal bounds, while when calculated using the comparative C_T method (as in Cantero et al. (2006)) the intervals have larger upper bounds due to being applied to an exponent. Significant changes are defined as those average fold changes with non-overlapping confidence intervals.

Primer sequences and full alignments

The sequences of important primers and the full alignment of CrACA1 to the Ca^{2+}-ATPase genes from Table 2.1 have been made available online as supplemental material at the Roux Lab *Ceratopteris* Research web page. This webpage is maintained for supplemental materials from our published papers and can be found at: http://www.sbs.utexas.edu/roux/Ceratopteris%20Page/ceratopteris_research.htm

Antibody design and development

Due to possible solubility issues with expression of a full length CrACA1, it was decided that a peptide fragment would be expressed in bacteria for use as an antigen. Based on the success of this method with the soybean Ca^{2+}-ATPase SCA1 (Chung et al., 2000), an analogous region of CrACA1 was chosen for this expression. Primers were

designed to amplify the A504-V596 region of the gene for expression using a pETBlue bacterial expression vector. The vector incorporates a His tag to allow for purification of expressed protein. The gene fragment was successfully sub-cloned into the pETBlue vector, expressed, and isolated. Crude induced extract was run over a Ni column for purification and eluted protein was concentrated using an acetone precipitation. The protein band of the expected molecular weight was sequenced by the ICMB Protein Facility (The University of Texas at Austin) and the sequence obtained exactly matched the start of the expected fragment. Column purified and concentrated protein was electrophoresed on a 4-15% polyacrylamide gel, the gel was stained and the band of the appropriate size was excised with a razor blade and moderately destained in a 1.5 mL ependorf tube. This gel slice was shipped to Pocono Rabbit Farm and Laboratory, Inc (Canadensis, PA) for solubilization (polyacrylamide can act as an adjuvant) and subcutaneous injection into Guinea pigs. Preimmune and first bleeds were obtained from two Guinea pigs, designated 1675 and 1676. Pig 1676 died of unknown causes before a third bleed could be obtained, but 1675 was collected until a terminal bleed was performed. Serums were aliquoted and kept frozen for use. Data presented here uses serum from pig number 1675.

Immunoblotting

The antibody serum was initially checked against uninduced and IPTG-induced crude bacterial preparations. A band of the appropriate size was recognized in both preparations, but was significantly stronger in the induced fraction. This band is not recognized by preimmune serum though there are some non-specific bands recognized by both sera.

Protein isolation and electrophoresis

A wide variety of protein isolation methods were attempted, including use of microsome buffers from the first step of a two-phase partitioning, buffer "EZ," straight SDS loading dye, and glass bead disruption buffer. Immunoblots presented here used the SDS loading buffer and glass bead disruption buffer methods. Testing showed that for microfuge tube isolation of proteins 40 mg of spores was an optimal amount.

The SDS loading buffer consisted of 50 mM Tris-Cl (pH 6.8), 2% (w/v) SDS, 0.1% (w/v) bromophenol blue, 10% (v/v) glycerol, and 100 mM β-mercaptoethanol (BME). BME was added just prior to use. Liquid nitrogen frozen spores with the germination liquid removed were ground with a mortar and pestle. The frozen powder was scraped into microfuge tubes and 200 µL of loading dye added. The material was immediately boiled for 5 minutes and loaded onto an acrylamide gel for electrophoresis. Every effort was taken to keep the spores frozen until the moment of boiling.

The glass bead disruption buffer consisted of 20 mM Tris-Cl (pH 7.9), 10 mM $MgCl_2$, 1 mM EDTA, 5% (v/v) glycerol, 0.2 M ammonium sulfate. Samples of spores were frozen with liquid nitrogen in microfuge tubes containing 100 µL of buffer and kept at -70 °C until all were ready for isolation. 1% BME (v/v) and 2X SIGMA*FAST*™ protease inhibitor (Sigma-Aldrich, St. Louis, MO) was added after thawing on ice and the spores were ground in the microfuge tubes using plastic pestles and a battery-operated hand grinder. 300 µL of buffer with 1% BME, 1X protease inhibitors, and 1% SDS was added to each sample and boiled immediately for 5 minutes. Samples were centrifuged for 10 minutes to pellet debris and loading buffer was added for gel loading.

Electrophoresis was performed using pre-cast commercial 5-15% or 5-20% gradient gels (Bio-Rad Laboratories, Inc., Hercules, CA or NuSep, Inc., Austell, GA). 4 or 7 µL per lane of Precision Plus Protein™ standard (Bio-Rad) was used for molecular

weight reference as needed. Typical conditions involved running in SDS page buffer with an initial constant voltage of 80 V until samples fully entered the wells followed by 100 – 120 V until the dye front reached the bottom of the gel.

Immunoblot transfers used a semi-dry transfer apparatus and methanol/SDS (Towbin) transfer buffer. Pre-soaked gels were transferred onto nitrocellulose sheets at a constant current of ca. 98 mA for 1-2 hours. If needed, membranes were Ponceau stained to facilitate division into pieces for separate primary antibody exposures. Membranes were rinsed in PBS and then blocked for 1 hour in 1.5% blotto (1.5% w/v non-fat dry milk in PBS). Membranes were exposed over night with gentle rocking at 4 °C to pre-immune or immune serum as appropriate (1:1000 serum dilution in 1.5% blotto containing 0.1% Tween-20). Before addition of secondary antibody the membranes were rinsed briefly 3 times with PBS and then 3 more times for 5 minutes each with PBS + 0.1% Tween-20. Anti-Guinea pig secondary antibody conjugated as appropriate for the detection method was applied to the membrane in PBS + 0.1% Tween-20 for 1 hour at room temperature; milk blocking agent was omitted due to possible background issues from use with goat secondary antibodies. The membranes were rinsed extensively in plain PBS to remove residual Tween-20 before detection.

Detection of signal from immunoblots was carried out with chemiluminescence, infrared fluorescence, and alkaline phosphatase-precipitation methods. Immunoblots presented here used the chemiluminescence and precipitation methods. For chemiluminescence, a horseradish peroxidase labled anti-Guinea pig secondary antibody was used at a dilution of 1:20,000. Equal volumes of substrate and enhancer solutions (SuperSignal® West Pico Chemiluminescent Substrate, Pierce, Rockford, IL) were mixed just prior to application to the membrane. The membrane was incubated in the dark for 5 minutes and then placed in a cassette with undeveloped film for various times to get a

variety of exposure intensities. The precipitation method used an alkaline phosphatase conjugated anti-Guinea pig antibody at a dilution in 1:10,000 in just PBS (no Tween-20). 1-Step™ NBT/BCIP solution (Pierce, Rockford, IL) was applied to a rinsed membrane and the solution changed every 30 minutes until band intensities were sufficient, at which point the membrane was washed with water to stop the development reaction.

Calcium-pumping ATPase activity

An established assay of Ca^{2+}-ATPase activity is through growth rescue of mutant yeast. Yeast strain K616 (*pmr1, pmc1, cnb1*) lacks endogenous Ca^{2+}-ATPase (PMR1 and PMC1) and Ca^{2+}/anion exchange activities and so exhibits limited growth on calcium depleted medium. K616 yeast were transformed using a PEG/Li-acetate/TE (PLATE) solution using 1 μg of pYES2, pYES2·NTD, or pYES2·NTD2 with 100 μg of syringe-sheared salmon sperm DNA as the carrier DNA as described by Elble (1992). Briefly, a small batch of PLATE was prepared by combining 9 mL 45% PEG 3,350, 1 mL 1M Li-acetate, 100 μL 1M Tris·HCL pH 7.5, and 20 μL 0.5M EDTA. 0.5 mL of freshly mixed PLATE was added to the pelleted yeast cells from 0.5 mL of overnight culture and vortexed. The DNAs were added to the cell and PLATE mixture, vortexed, and allowed to incubate on the benchtop overnight. 50 μL of this was spread the next morning on selective media (YNB -Ura) plates.

Colonies were picked and re-streaked 4 days later on selective media plates and grown for another 4 days. Individual colonies from the second streak were used for preparing freezer stocks. Growth rescue was assayed by streaking untransformed, pYES2, pYES2·NTD, and pYES2·NTD2 containing K616 yeast along with a wild type strain onto separate quarters of the same YNB – Ura + 10 mM EGTA selective plates, which contained either raffinose or raffinose + galactose as the carbon source. Positive Ca^{2+}-ATPase activity is indicated by growth of the pYES2·NTD or pYES2·NTD2 K616

yeast on the galactose plates and no or limited growth on the raffinose only plates due to the presence of EGTA.

RESULTS

Sequence information and alignments

Translated query BLAST searches (blastx) matched EST Cri2_7_N15_SP6 (Accession BE643069) from the initial batch of EST sequences to calcium pumping ATPases in *Oryza sativa* and *Hordeum vulgare*. Additional sequencing of the EST indicated that only the extreme 3' end of the full length cDNA had been captured. Chromosome walking obtained the rest of the sequence, designated CrACA1 (for *C. richardii* autoinhibited Ca^{2+}-ATPase) (accession number AY333123). Inputting the full sequence of CrACA1 into a blastx search returns strong identity to Ca^{2+}-ATPases from a variety of plant species (Table 2.1). As can also be seen in Table 2.1, the amino acid identity of *CrACA1* to distantly related plant species is quite high, coming in at near 50% identity overall.

Alignment of CrACA1 to the same sequences listed in Table 2.1 highlights several primary sequence characteristics common to ATPases (Figure 2.2). The overall organization of Type II ATPases consists of 10 transmembrane regions (numbered M1 through M10) with two large cytoplasmic loops designated "Region B" and "Domain C." A WoLFPSORT prediction (Horton et al., 2006) of the translated amino acid sequence anticipates that CrACA1 contains 10 transmembrane domains and will be localized to the cell periphery with its N-terminal end facing inward. Computational methods for identification of transmembrane regions are not entirely accurate, but there is strong

amino acid identity in the potential transmembrane domains, improving the likelihood that CrACA1 is structured similarly.

There are several conserved sequences of note from the alignments. The sequence DKTGTLT is strongly conserved as a site of phosphorylation (at the aspartate residue) and is present at position 489 of CrACA1; as can be seen in the alignment, this sequence is present and identical in all 15 sequences compared. There is also a 23 amino acid "hinge" sequence consisting of VAVTGDGVNDSPALKKADIGVAM to which CrACA1 has 18 identical amino acids. Narrowing the comparison of the hinge sequence to AtACA8 through 10, there are only 2 differences, with CrACA1 being different from the majority at only one site. Another short but highly conserved sequence, PEGL, is located in M4 and is present as well in CrACA1. The PEGL sequence is followed by a well-conserved 40 amino acid sequence connecting to the aforementioned phosphorylated aspartate residue. Similarly, CrACA1 has an elongated N-terminus (as compared to animal types) which implies that it may also have the calmodulin-regulated autoinhibitory domain. This region has several key amino acid identities at positions referred to as 1, 5, 8, and 15 (Geisler et al., 2000) but helical wheel analysis of the region did not have an archetypical arrangement.

Phylogenetic analysis of CrACA1 compared to the proteins from Table 2.1 indicate that CrACA1 is most similar to the plasma membrane localized Arabidopsis Ca^{2+}-ATPases ACA8, 9, and 10 (Figure 2.3). As well, twenty one of CrACA1's twenty seven "nearest neighbors" from the WoLFPSORT prediction are plasma membrane localized.

ATPase activity assay

Transformed K616 yeast strains will grow on YNB plates with URA drop out supplement with glucose but no strains grow on those containing galactose as the sole

carbon source. Growth of all +URA strains was obtained on 2% raffinose plates and growth on galactose could be achieved with inclusion of 1% raffinose to the media. Wild type and K616 transformed with pYES2·NTD2 were the only strains to grow on the galactose + raffinose plates containing 10 mM EGTA (Table 2.2), indicating that the N-terminal deletion protein of CrACA1 is capable of *in vivo* Ca^{2+}-ATPase activity.

RNA expression profile

The relative RNA expression levels of CrACA1 were examined via real-time RT-PCR (Figure 2.4). CrACA1 is transcribed before light exposure, but shows a drop off in expression afterwards. Six hours after light exposure RNA levels are not statistically significant from zero, but levels continue to fall and are significantly lower by 9 hours. Expression appears to level off at about one-fifth of starting amounts by 15 hours and remains stable at this amount through 24. The larger confidence intervals at the earlier time points are indicative of higher variation in the measurements, later time points are much more consistent.

Protein expression

Recognition of a protein band of expected size (ca. 125 kD) was achieved once using the liquid nitrogen isolation method (Figure 2.5 A). A repeated immunoblot using the same samples kept frozen at -70 °C showed a loss of the large band and an appearance of lower molecular weight bands. Based on this, the bands seen in Figure 2.5 B are assumed to be cleavage products from the full length CrACA1. This qualitative immunoblot indicates that CrACA1 protein levels are present through 24 hours.

DISCUSSION

Data available at the start of my project pointed to the Ca^{2+} flux being the major determinant of spore polarity fixation. Of the two potential components of the flux, Ca^{2+}-ATPases were the most attractive, having ample characterization and available sequence information in other plant systems. Indeed, a fragment of a Ca^{2+}-ATPase was represented in our first batch of ESTs sequenced from the 20-hour spore library, which had the added bonus of indicating that at least one Ca^{2+}-ATPase was being expressed at that early time. Calcium channels, specifically of the mechanosensitive variety were also attractive subjects, but the lack of any identifiable plant sequences made studying them in our own system problematic. As well, the majority of information regarding calcium channels in plants has been based on patch clamping techniques, a methodology that would have been problematic in the spores of *Ceratopteris* due to the spore coat. Protoplast regeneration would have been difficult as well due to the considerations of regeneration and timing of gravity responsiveness.

The first cloned Ca^{2+}-ATPase from *C. richardii* was compared to Ca^{2+}-ATPases from other plant systems, specifically those that have been localized to the plasma membrane (PM). In order to be a component of the spores' calcium efflux, the *Ceratopteris* version would have to be of the PM variety. Limitations in imaging at the early stages of spore development make it extremely difficult to localize. Therefore I chose to analyze the sequence of CrACA1 and relate it to information gathered on Ca^{2+}-ATPases from other, more amenable systems. In order to have relevance to gravity-directed spore polarity, it was important to show that not only is the RNA message CrACA1 expressed at the time of gravity fixation, but that the protein is present as well. To that end, real-time RT-PCR was selected as the method of choice for examining the

early RNA expression profile and an antibody was raised to compare RNA and protein expression over similar time frames.

Gene sequence analysis

Moller et al. (1996) list three common components of P-type ATPases, high sequence identity, presence of certain sequence motifs, and similar hydropathic profiles. Overall identity of *CrACA1* to higher plant PM Ca^{2+}-ATPases is quite high, at around 50% (Table 2.1), with specific regions having much higher similarity. All of the BLAST returns on Table 2.1 had an expect value of 0.0, indicating the extremely high probability of the match. The major regions of similarity are the putative transmembrane regions and the common motif regions (Figure 2.2). The major motifs of P-type Ca^{2+}-ATPases are present in *CrACA1*, several of which are specifically noted in Figure 2.2. Overall gene structure appears to be similar in regards to organization and number of transmembrane regions and catalytic cytoplasmic loops indicating a similar arrangement of hydrophilic and hydrophobic regions. Additionally, the WoLFPSORT analysis also predicts that CrACA1 would localize to the plasma membrane, and 21 of 27 "nearest neighbors" are plasma membrane localized themselves. Phylogenetic analysis groups CrACA1 with known plasma membrane Ca^{2+}-ATPases (Figure 2.3), further increasing the likelihood of PM localization for CrACA1. With all of this matching information it is highly likely that CrACA1 is a legitimate PM Ca^{2+}-ATPase from *C. richardii*.

It has been shown that Arabidopsis and soy Ca^{2+}-ATPases can successfully rescue the growth of the K616 yeast strain (Harper et al., 1998; Chung et al., 2000). Confirmation of CrACA1's Ca^{2+}-ATPase activity has been achieved using this same assay (Table 2.2). Sequence similarities along with confirmation of *in vivo* activity is strong confirmation that CrACA1 is indeed a functional Ca^{2+}-ATPases.

Expression profiling of CrACA1

If CrACA1 has a unique role in the polarity establishment or polar axis alignment of the germinating spore it could be reflected in the timing of gene expression. At a minimum the gene and gene product would need to be expressed during the time of the gravity-associated calcium efflux that occurs during the window of polarity fixation. Real-time RT-PCR was chosen to examine the RNA levels and a custom antibody was raised for analysis of the protein product.

Real-Time RT-PCR

As discussed in the introduction, there are several details to be concerned with in regards to qPCR. The LUX™ primer system (Figure 2.1 D) was selected as the detection method, it being a good balance of sensitivity, accuracy, and cost. Of the four tested control genes, APT1 and α-tubulin were determined to be satisfactory and the presented data (Figure 2.4) uses APT1 as the reference gene. The remaining major issue is that of data analysis. Since cycle thresholds are dependent upon both starting templates and reaction efficiencies, care must be taken to compensate for both of these variables. The careful selection and use of control/reference genes compensates for both of these factors. Of the two calculation methods for determining the relative gene expression changes, the ΔC_T method could not be used with *CrACA1* due to the differences in PCR reaction efficiencies between it and APT1. The standard curve method was used instead, whereby the C_T values are normalized to a reference curve constructed from serial template dilutions. As well, I applied a statistical analysis method, a two-tailed distribution formula, to the data processing to generate meaningful data. This method is ideal because it generates confidence intervals based on sample size and standard deviations. Most previously published qPCR results were reported simply with standard errors and no commentary on what changes were statistically significant. With confidence intervals,

significance is easily determined visually, but more importantly alterations in expression can be more accurately examined. Rather than limiting ourselves to expression changes being significant based on magnitude we can look for consistent changes in expression patterns. I applied this method to a study published in collaboration with other members of the Roux lab (Cantero et al., 2006).

Figure 2.4 shows the RNA expression profile for *CrACA1* over the first 24 hours after light exposure. As can be seen, RNA levels drop during early spore germination ending at a point that is five-fold less than in spores not exposed to light (0 hour). Until 12 hours the spores maintain a fairly steady amount of *CrACA1* message, the changes from 3 until 12 hours are not statistically different although 3 hours is different from 0. From this pattern it appears that after around 12 hours *CrACA1* expression becomes less important for the spore development. *CrACA1* is present at a steady state levels 15 hours and beyond, likely due to involvement in basic calcium homeostasis at those times. The confidence interval differences between 0-12 and 15-24 hours are of note. The broader confidence intervals indicate greater variability in the data from spores at the earlier time points. The same trend was noted in four of the six qPCR results from Salmi et al. (2005). This could be indicative of variability in the population which is mirrored in population percentages showing correct gravity alignment when spores were rotated 180° at varying times (Edwards and Roux, 1994). Although pre-soaking the spores in the dark for 5 days increases spore synchronicity, spore behavior is not completely locked. The process of initiating germination likely involves a large number of changes within the spore, and, with *CrACA1* and other genes as indicators of the general state within the spore, early germination is a turbulent time.

Immunodetection

The immune serum raised to a bacterially expressed fragment of CrACA1 detects both the original fragment as well as discreet and unique protein bands from *C richardii* isolate. Detecting a band of the expected size proved to be exceedingly difficult. Based an the sample shown in Figure 2.5 A and the same sample run at a later time point, the lower molecular weight bands most often detected were likely degradation products. Due to the variety of isolation methods attempted, it is assumed that CrACA1 is simply prone to cleavage during the isolation process. The immune serum can detect the presence of specific bands through 24 hours, which matches the continued expression of RNA through the same time point.

SUMMARY

The first cloned Ca^{2+}-ATPase from *C. richardii*, CrACA1, has high primary sequence similarity to other known plant Ca^{2+}-ATPases, specifically a subset of Ca^{2+}-ATPase from *Arabidopsis* that are known to localize to the plasma membrane. The RNA and protein are present during the first 24 hours after light-initiated germination begins. Its presence during the polarity fixation process makes it an excellent candidate for further analysis for the role of Ca^{2+}-ATPases in the polarity fixation process. The major contributions of the presented work are from the addition of a non-standard plant system's Ca^{2+}-ATPase to the available database as well as an improved method for the statistical analysis and presentation of qPCR data.

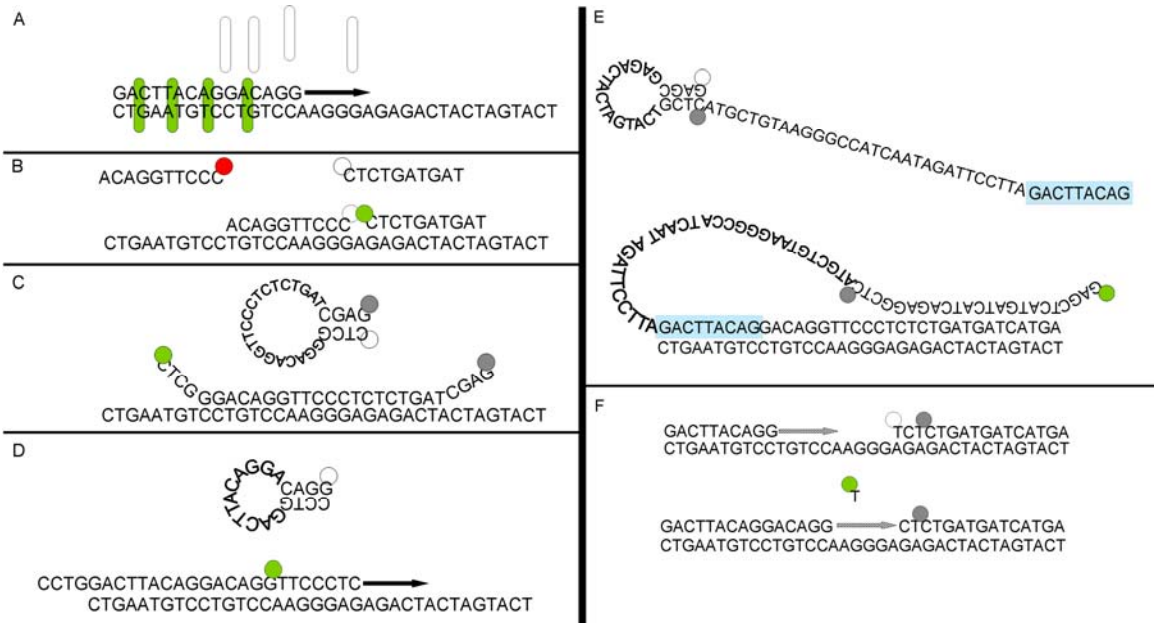

Figure 2.1: Various methods of quantitative real-time RT-PCR.

Green circles represent the actively fluorescent compound being detected in each case. Empty circles represent quenched or non-fluorescent moieties. Grey circles represent quenching compounds. A. Double Stranded DNA binders such as SYBR® Green. Binding to double stranded product causes a compound to become fluorescent. The arrow represents the extension of a PCR primer by polymerase. B. LightCycler™ FRET activated fluorescent primers. Unbound LightCycler™ primers on top. The left primer is fluorescent when unbound, represented by red circle. When both primers are bound to the target (lower) FRET occurs and excitation of the first fluorochrome causes emission from the second which is detected by the PCR machine. C. Molecular Beacon. Unbound probe has hairpin structure (top) that keeps the quencher near the fluorochrome, preventing fluorescent emission. Binding to the target (lower) spatially removes the quencher from the fluorochrome thereby allowing fluorescence. D. LUX™ type primers. Hairpin structure of the primer quenches the fluorescent signal. Incorporation of the primer into the extending product increases fluorescent signal. The arrow represents the extension of a PCR primer by polymerase. E. Scorpions®. The blue box represents the primer portion of the Scorpion®. The hairpin at the end acts much like the Molecular Beacons, keeping the quencher in proximity to the fluorochrome. Scorpions® get incorporated into the product as primers and fluorescence occurs when Scorpion® tail binds to the same strand that the primer became incorporated into, thereby separating the quencher form the fluorochrome and allowing emission. F. TaqMan® type. Fluorochrome and quencher on the probe are in close proximity (top). As the polymerase exonuclease activity (represented by the striped arrow) approaches the probe its 5' exonuclease activity cleaves the probe releasing the fluorescent moiety from the quencher (bottom) and allowing fluorescence emission. Originally appeared in (Salmi et al., 2006).

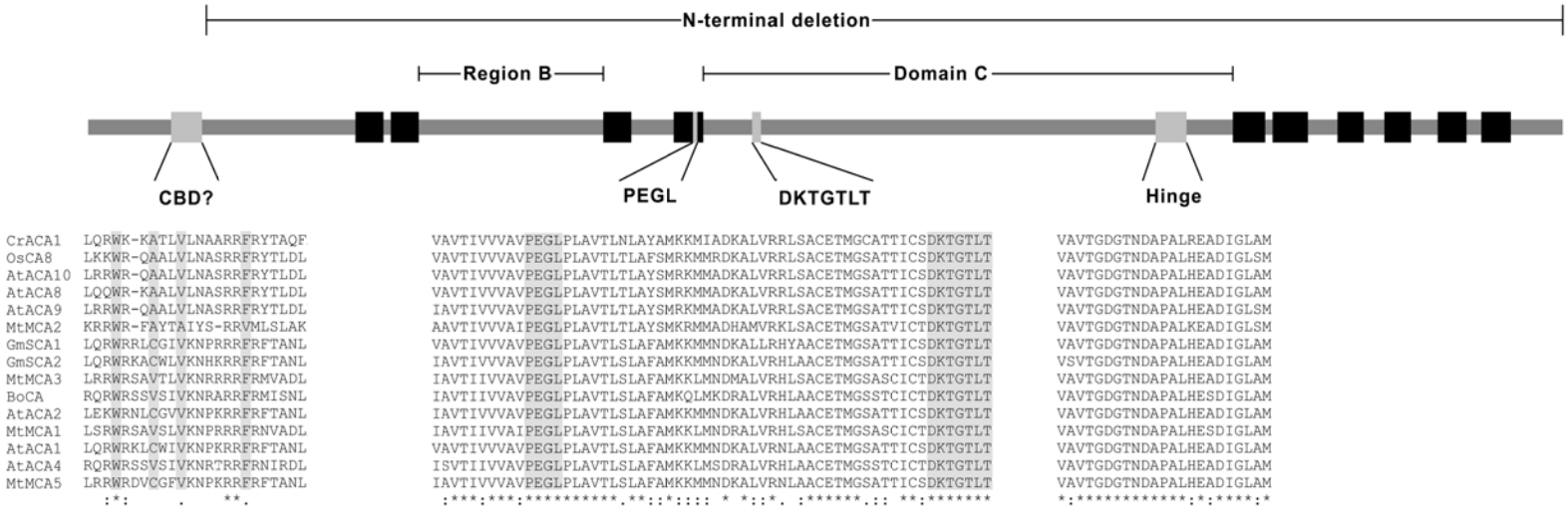

Figure 2.2: CrACA1 sequence overview and selected alignments.

Organization and conserved features of CrACA1 are indicated in proportional scale. Named regions and the span of the N-terminal deletion are indicated. Dark boxes represent putative transmembrane regions. Light boxes are conserved regions with the accompanying sequence alignments from Clustal W listed below. For the alignments, asterisks denote fully identical amino acids, double dots indicate the presence of conserved substitutions, and single dots are semi-conserved. Shaded residues are from conserved regions discussed in the text. Aligned genes are those from Table 2.1. Full sequence alignments can be found in the online supplemental materials.

Table 2.1: Selected protein sequences matching to CrACA1.

The nucleotide sequence of CrACA1 was used for a translated BLAST query (BLASTX). Presented here are a sample of those returned sequences with an e = 0.0. Identity is based on exact amino acid matches, positives are based on identical or conserved amino acid substitutions. Genes are presented in order of highest percent identity. Double letter prefixes denote the species the specific Ca^{2+}-ATPase sequence is from: Os = *Oryza sativa*, At = *Arabidopsis thaliana*, Mt = *Medicago truncatula*, Gm = *Glycine max*, Bo = *Brassica oleracea*

Abbreviation	Accession number	Identity		Positives	
OsCA8	NP_001053795	601/1061	56.6%	766/1061	72.2%
AtACA10	NP_194719	579/1044	55.5%	749/1044	71.7%
AtACA8	NP_851200	580/1051	55.2%	760/1051	72.3%
AtACA9	NP_188755	581/1068	54.4%	750/1068	70.2%
MtMCA2	AAL17950	497/960	51.8%	678/960	70.6%
GmSCA1	AAG28435	502/1023	49.1%	682/1023	66.7%
GmSCA2	AAG28436	502/1025	49.0%	684/1025	66.7%
MtMCA3	AAL73984	502/1028	48.8%	690/1028	67.1%
BoCA	CAA68234	490/1017	48.2%	681/1017	67.0%
AtACA2	NP_195479	489/1019	48.0%	671/1019	65.8%
MtMCA1	AAL17949	491/1026	47.9%	683/1026	66.6%
AtACA1	NP_849716	489/1029	47.5%	676/1029	65.7%
AtACA4	NP_181687	485/1022	47.5%	685/1022	67.0%
MtMCA5	AAM44081	482/1018	47.3%	659/1018	64.7%

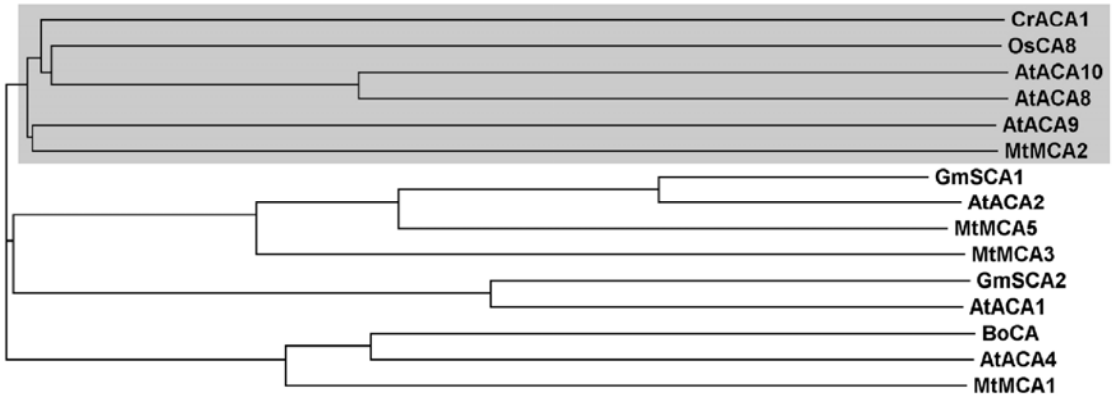

Figure 2.3: Phylogenetic Phylip Tree based on the translated sequence of CrACA1.

The genes listed in Table 2.1 were aligned and a phylogenetic tree generated using Clustal W. The major branching containing CrACA1 (blocked in gray) includes three *Arabidopsis thaliana* Ca^{2+}-ATPases known to localize to plasma membranes.

Table 2.2: Growth rescue assay for Ca^{2+}-ATPase activity.

Wild type strain Y187 and both transformed and untransformed K616 mutant yeast were streaked onto partitions of YNB – Ura selective media plates that were either inducing (2% galactose) or non-inducing (2% raffinose only). Ca^{2+}-ATPase activity was assayed for by growth on inducing plates in the presence of 10 mM EGTA. The two N-terminal deletion (NTD) constructs differ in the start codon. NTD is a simple ATG while NTD2 utilizes a Kozak consensus sequence. Yeast were allowed to grow at 30 °C for 5 days. Growth was scored as robust (++), colony forming (+), or non-colony forming (-).

	2% Raffinose	1% Raffinose 2% Galactose	2% Raffinose 10 mM EGTA	1% Raffinose 2% Galactose 10 mM EGTA
Y187 (WT)	++	++	++	++
K616	-	-	-	-
+pYES2	++	+	-	-
+pYES2·NTD	++	+	-	-
+pYES2·NTD2	++	+	4 colonies	+

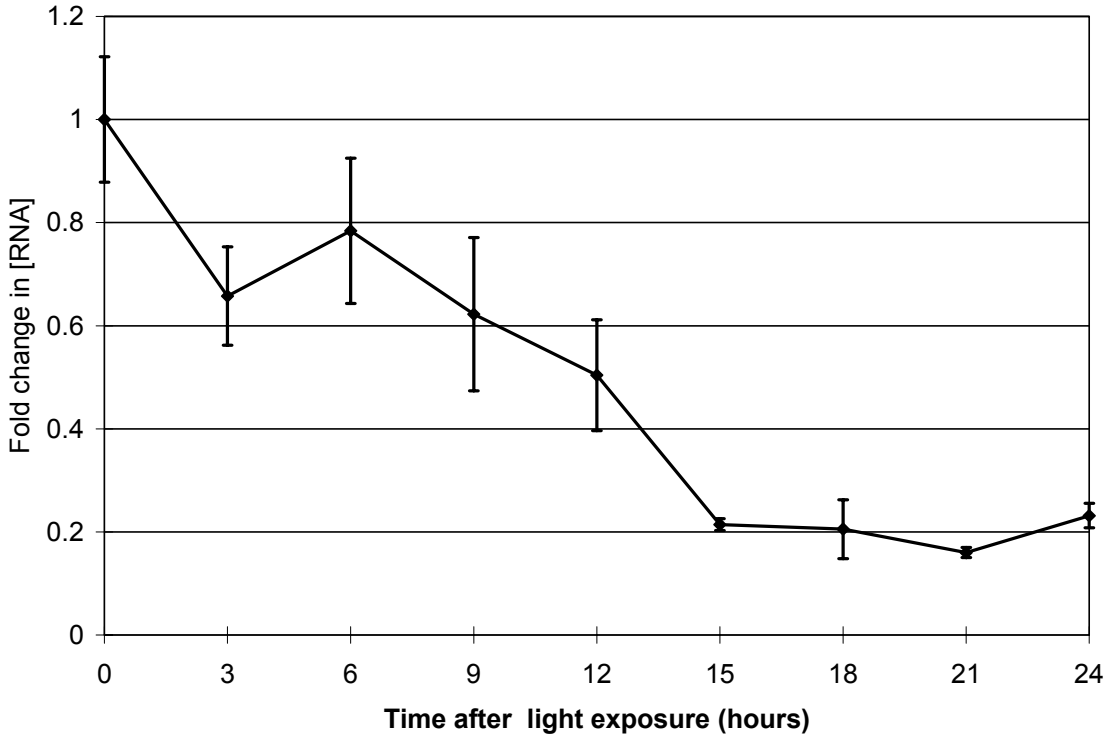

Figure 2.4: Early RNA expression of CrACA1 in germinating spores.

RNA was isolated from spores collected every three hours after light exposure until 24 hours. Real-time RT-PCR was performed using the LUX™ primer system with APT1 as a reference gene. Changes in concentration were normalized to hour 0 using the standard curve method. Error bars represent 95% confidence intervals calculated as described in Materials and Methods, non-overlapping intervals indicate statistically significant expression level differences.

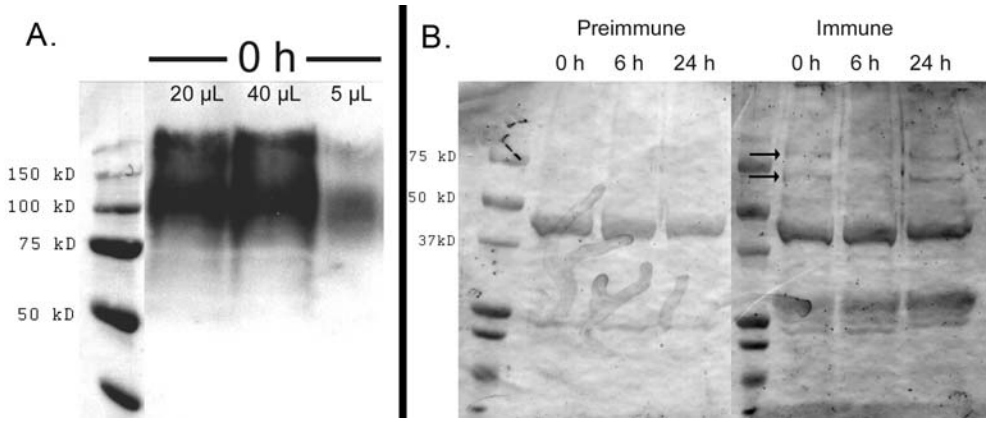

Figure 2.5: Selected immunoblot results.

Immunoblot results from two isolation methods. A. Recognition of a band of expected size from crude protein extracted from spores ground without buffer in liquid nitrogen then boiled in SDS sample buffer. Loaded lanes from left to right have 20 µL, 40 µL, and 5 µL of crude extract loaded. B. Qualitative immunoblot for the smaller fragments during the first 24 hours post light exposure. Spore samples were frozen in grinding buffer at the indicated times post light exposure. Thawed samples were processed simultaneously by grinding in buffer lacking SDS and then boiling for 5 minutes after addition of SDS. Left half was pre-immune serum, right half was immune. The bands unique to immune serum are indicated with arrows and run just above and below the 75 kD molecular weight marker.

Chapter 3: Pharmacological Modifications of Ca^{2+}-ATPases

INTRODUCTION

Calcium in Polarized Growth[2]

The research presented here is primarily focused on helping to decode the role of Ca^{2+} in gravity-directed polarity establishment of single plant cells. However, calcium functions in a vast array of biological processes in diverse organisms from bacteria to mammals. The localization, frequency, duration, and intensity of calcium signals are believed to encode the information required for independently regulating a multitude of cellular activities. In the case of spores of the fern *Ceratopteris richardii*, calcium can function in the establishment of growth polarity. Unlike some other fern spores that have been examined, *C. richardii* spores align their initial rhizoid growth with the gravity vector (Edwards and Roux, 1998). The occurrence of a calcium current that flows into the bottom and out the top of the spore coincides with the period during which gravity determines the direction of cell polarization (Chatterjee et al., 2000), and the direction of this current is rapidly responsive to changes in orientation (Stout et al., 2003; Salmi et al., 2007). This polarized calcium current subsides after about 24 h, but its direction predicts the alignment of subsequent gravity-directed cellular processes, namely nuclear migration, asymmetric cell division, and primary rhizoid emergence. Inhibition of this current by the calcium channel blocker nifedipine results in suppressing the ability of the emerging rhizoids to orient relative to gravity (Chatterjee et al., 2000). This implies a role for calcium in organizing the fern spore for asymmetric development.

[2] Portions of this section are my own work taken from Bushart and Roux (2007).

Germinating fern spores have commonalities with other systems, most notably pollen. The germination of both pollen and fern spores results in the emergence of a cell—pollen tube from pollen; rhizoid from spore—that grows in a polar fashion, primarily at its apical end. In both of these tip-growing cells, the delivery of secretory vesicles to the growing end is guided in part by a calcium gradient, with calcium entering at the tip where it is most highly concentrated. Calcium is clearly involved in the early stages of pollen germination and pollen tube growth, as has been very well documented in the literature, making it worth examining what is known about calcium dependent pollen growth and development for comparisons back to the *C. richardii* system (for a comprehensive review of ions in pollen see Holdaway-Clarke and Hepler (2003)).

The polarized growth of emerging pollen tubes is crucial to proper fertilization, although, rather than gravity, pollen uses positional signals from the stigma and style as initial growth guides. Calcium is required in the growth media for proper spore rhizoid and pollen tube elongation, but pollen also requires exogenous calcium for germination to occur at all. Chemical inhibition of calcium channels will block the germination of pollen (Bednarska, 1989; Malho et al., 1994; Franklin-Tong et al., 2002; Wang et al., 2004), certain calmodulin-binding proteins are necessary for germination (Golovkin and Reddy, 2003), and cation influx is predictive of the aperture where the pollen tube will emerge (Weisenseel et al., 1975). A strong uptake of calcium at the site where polarized growth begins has also been observed in algal zygotes (Berger and Brownlee, 1993; Pu and Robinson, 1998) and root hairs (Wymer et al., 1997). In the case of *C. richardii* fern spores, which only have a single point of exit through the spore coat, the early site of calcium uptake predicts the direction of post-emergent rhizoid growth (Chatterjee et al., 2000). The channels involved in germination and tube growth in pollen appear to at least be of the same type (Wang et al., 2004), most probably stretch-activated calcium

channels, as indicated by patch clamping and the inhibition of calcium entry into pollen tube protoplasts by a spider venom that blocks stretch-activated channels in animal cells (Dutta and Robinson, 2004). The importance of general calcium homeostasis is also indicated by the requirement of the plasma membrane calcium pump ACA9 for proper germination and fertilization to occur (Schiott et al., 2004).

There is abundant documentation on the role for calcium in tip growth. A variety of imaging and measuring methods have repeatedly shown that growing pollen tubes have a high concentration of calcium and calcium influx at their tips (Malhó et al. 1994; Pierson et al., 1994; Malhó et al., 1995; Malhó and Trewavas, 1996; Franklin-Tong et al., 1997; Holdaway-Clarke et al., 1997; Messerli and Robinson, 1997; Camacho et al., 2000; Snowman et al., 2000; Camacho and Malhó 2003; Franklin-Tong et al., 2002; Lazzaro et al., 2005). Scheuerlein and colleagues previously used fura-2 to visualize the accumulation of Ca^{2+} at the growing tip of fern rhizoids, the results of which are shown in Bushart and Roux (2007).

Beyond the simple establishment of the tip-associated calcium concentrations, research on this topic has also given us information on the impact of the ion on growth control (see reviews Battey and Blackbourn, 1993; Franklin-Tong, 1999; Feijo et al., 2004; Hepler 2005). As a brief summary, pharmacological inhibition of calcium channels inhibits the emergence of pollen tubes, just as it inhibits the emergence of rhizoids. In pollen, the tip accumulation of calcium dissipates after cessation of growth, manipulation of calcium sources and ionophores can redirect tube growth, and waves of calcium accumulation are correlated with pulses in growth. The actual effectors of these tip-associated calcium events are still being decoded, likewise for the role of Ca^{2+} in gravity-directed polarity establishment.

Chemical Inhibition of Ca^{2+}-ATPases

In order to dissect the role of the calcium efflux in spore polarity, chemical agents were selected that could specifically inhibit either the plasma membrane or endomembrane Ca^{2+}-ATPase activity. The developed antibody serum to CrACA1 is unsuitable for this function since the available epitope would be on the cytoplasmic side. Among the possible choices for chemical inhibitors, 2,5-Di-(*t*-butyl)-1,4-hydroquinone (BHQ) and 2′,4′,5′,7′-tetrabromofluorescein (Eosin Y or EY) were chosen.

BHQ is a member of the dihydroxybenzene/hydroquinone family of sarco/endoplasmic reticulum Ca^{2+}-ATPase (SERCA) inhibitors. BHQ inhibits SERCA pumps in a similar but distinct fashion to the archetypal sesquiterpene lactone family member, thapsigargin. Analysis of these two classes of compounds indicate that they have separate binding sites yet impair Ca^{2+} binding by shift of the enzyme to the E2 conformational state (Khan et al., 1995). Since the end results are equivalent, BHQ was selected as the inhibitor of choice for the SERCA class of pumps due to its lower cost, a point of consideration due to the large volumes of inhibitor solutions required for the liquid-exposed, fixed-orientation polarity experiments.

EY is a fluorescein derivative, a class of compounds known to bind to Ca^{2+}-ATPases in an inhibitory manner. De Michelis et al. (1993) demonstrated a 10,000 fold higher specificity of EY for plasma membrane Ca^{2+}-ATPases over H^{+}-ATPases. EY is also more effective than other fluorescein dervatives such as erythrosin B (De Michelis et al., 1993), even at sub-micromolar levels and within 30 minutes of application (Beffagna et al., 2000; Romani et al., 2004). The high activity and specificity for the PM Ca^{2+}-ATPases made EY the best choice for inhibition of the PM Ca^{2+} efflux.

Together, BHQ and EY can be used to compare the relative importance of endo- or plasma membrane Ca^{2+}-ATPases by selectively inhibiting the function of one or the

other. If the efflux of calcium from the spore is critical for polarity development, we would expect that inhibition of PM Ca^{2+}-ATPases via EY would depress downward rhizoid emergence while SERCA inhibition might have indirect effects via alterations in available calcium stores. It is also possible that PM Ca^{2+}-ATPases may simply be acting downstream of calcium uptake, serving to maintain a certain level of Ca^{2+} homeostasis. In that case, we would expect only channel inhibitors to impact gravity-directed spore polarity and Ca^{2+}-ATPase inhibition should only affect general cell growth.

Connecting the calcium flux to polarity establishment through real-time flux measurements

The main purpose of my investigations has been to connect the early spore calcium flux to the polarity axis alignment in a more concrete manner. The use of inhibitors of components that may be involved in this process can provide some initial insights, but we need to confirm that not only do these drugs impact eventual axis orientation, but that they are initially modifying the calcium flux in a meaningful way. Although there are a number of visualization and measurement techniques that would answer this, few would be successful with the *Ceratopteris* spore system.

Patch clamping is a technique used extensively for the measurement of the electrochemical behavior of cell membranes. The alteration of calcium, and specifically calcium channel activity, would be detectable with patch clamp techniques. However, these types of assays require direct contact with the membrane, which is not possible using intact spores due to the spore coat. One could use regenerated protoplasts for this, but the percentage of regenerating cells is only 0.4% of plated protoplasts (Edwards and Roux, 1998) and there is no easily identifiable marker for locating them.

There are a number of visualization techniques that have been employed in other systems. Certain techniques such as the aequorin system are not viable due to needing a

transgeneic organisim expressing the apoaequorin or the problems of loading exogenous proteins. As mentioned above, several labs have used indicators to demonstrate real-time changes in Ca^{2+} concentrations in plant cells in response to a number of different stimuli. These indicators are unacceptable due to the high and broad spectrum of auto fluorescence from the spore coat. There also exists an issue with resolution since many methods may be good at the tissue level, but not specific enough for sub-cellular localizations. External indicators are a possibility if the spore coat itself could be masked, but this avenue was not pursued since we already had experience using ion selective probes for external calcium measurements.

At the start of my project, the available method for measuring the Ca^{2+} current used a single oscillating electrode that was capable of measuring a single spore's response. Probes like this measure electrical potential changes using glass electrodes filled with an ion selective substance to give it specificity. This was used effectively to sketch out the initial calcium flux of the spores (Chatterjee et al., 2000) and then more recently to try and refine the time frame in which a spore can respond to a change in orientation (Stout, 2004). A probe like this is useful but still limited. Due to the careful positioning needed with the glass tip probe, the apparatus is not capable of constant measurements during positional changes of the spore. As well, it can only measure one spore at one position at a time, increasing variability in conditions and making it time consuming to get multiple measurements of the same time point. Marshall Porterfield and Stan Roux worked to remedy these shortcomings through design of a lab-on-a-chip type device.

ul Haque et al. (2006) developed an *in silico* cell electrophysiology biochip (referred to as the CEL-C system) in order to address the issues of measuring calcium fluxes of multiple cells, at multiple points, and in real time. The CEL-C biochip consists

of a silicon microchip containing sixteen pores in which individual spores can be loaded. Each pore has four Ag/AgCl electrodes for measurement of calcium fluxes at points every 90° around the circumference of a spore. Since the spores are placed in position with the electrodes and kept in position for the length of the experiment, the whole unit can be rotated in any fashion without interruption in recordings. With sixteen available pores, sixteen individual spores from the same batch and same developmental time point can be simultaneously measured while experiencing roughly the same conditions. This system was selected for measuring the effects of Ca^{2+}-ATPase inhibitors because of this high-replicate ability, similarity to previously used electrode techniques, and ease of use.

MATERIALS AND METHODS

Plant Materials and Experimental Conditions

To maintain media consistency across replicates, batches of half-strength Murashige and Skoog (MS) basal medium (Sigma-Aldrich, St. Louis, MO), pH 6.3 were made in large enough volumes for use in all conditions for all rinses required for one experiment. The medium was divided into smaller vessels as necessary for convenience of use and for addition of drugs.

Batches of 10 to 15 mg of *C. richardii* Hn-n spores were surface sterilized as described in Edwards and Roux (1998). Spores were soaked with sterile distilled water in darkness for a minimum of 5 days. In indicated cases drugs were added to the soaking media at the identified times. Upon light exposure, spores were embedded in half-strength MS medium, pH 6.3, with 1% agarose at a concentration of approximately 1 mg spores per mL of medium. For certain treatments, drugs were included in the agarose solutions. Agarose integrity and spore directionality during growth were maintained by

sowing 0.4 mL of the spores in the agarose medium onto strips of 500 micron monofilament nylon mesh (Small Parts, Inc., Miami Lakes, FL) resting on a supportive backing of clear transparency film. Both the mesh-sown spores and the supportive backings were placed into 15 mL screw top conical tubes containing 10 mL of the appropriate treatment medium. Spores were allowed to grow in a fixed vertical orientation for 3 days in a growth cabinet at 29°C under continuous light. Tube position in the holding racks was random and randomly altered during media changes or at least once per 24 h.

Drug Preparation and Use

2,5-Di-(*t*-butyl)-1,4-hydroquinone (BHQ) (Calbiochem, La Jolla, CA) was dissolved in 100% dimethyl sulfoxide (DMSO) or 100% ethanol to make a 0.1M stock solution. The stock solution was used full strength or diluted with 100% solvent so that final concentrations of the drug could be made by adding 1 µL per 1 mL of growth medium. Solvent was added to control tube medium at a matching concentration of 0.1%. Drug-containing media were made in larger batches for division amongst the 15 mL conical tubes. Treatment media was added and removed at the indicated times post light exposure. Removal of the drug was aided by a rinse step consisting of soaking the spore strips in 10 mL of drug-free medium for at least 60 minutes. This was followed by an exchange for fresh medium for the remainder of the 3 days of growth.

The free acid form of 2′,4′,5′,7′-tetrabromofluorescein (Eosin Y, "H_2EY") (Sigma-Aldrich, Inc.) was treated in a similar manner to BHQ. A 0.2 M stock solution was made in 100% DMSO for direct or diluted use as above. The solubility of the free acid form limited final concentrations of EY in the ½ MS medium to 2 µM or less. The disodium salt form of EY (2′,4′,5′,7′-tetrabromofluorescein disodium salt, "Na_2EY") is water soluble and was used at final concentrations up to 100 µM. Stocks were prepared

as above but using sterile distilled water as the solvent. Untreated controls for Na_2EY used either unmodified ½ MS or, in experiments involving DMSO soluble drugs and controls, the number of necessary samples was limited by adding 0.1% DMSO to the Na_2EY treatments.

Scoring and Statistics

Directionality of rhizoid growth was scored visually under a microscope at 40x total magnification. Rhizoids were categorized according to the major growth direction in relation to a horizontal midline. Rhizoids below the midline were "down," rhizoids growing above were "up," rhizoids growing straight along the midline or crossing the midline multiple times were considered "midline," spores with more than one rhizoid were scored as "multiple." Any spore with no rhizoid or a rhizoid less than one spore diameter was considered to be "not germinated," therefore scoreable rhizoid percentages are not necessarily indicative of spore viability rates. For consistency with calculations from Edwards and Roux (1994) "% down" was calculated based on the number of "down" rhizoids versus "midline" and "up," which make up the population of spores considered to be non-gravity responsive. "Up," "down," "midline," and "multiple" were the pool of germinated spores for comparisons of germination rates.

Percent rhizoid emergence and downward rhizoid growth were calculated for each scored strip. Percentages of the same condition were grouped and averaged. A two tailed, two-sample unequal variance Student's t-Test was performed to determine statistical difference between control and treatment averages, using a cut off for significance of $p < 0.05$.

Real-Time Calcium Measurements

Measurements of calcium efflux from the spores were taken in real time using the CEL-C microchip system developed in D. Marshall Porterfield's laboratory at Purdue (ul Haque et al., 2006). The fabrication methods for the CEL-C lab-on-a-chip are outlined in the referenced paper, but the relevant features of the finished product are as follows. The spore-interface portion of the CEL-C consists of sixteen etched wells each with four Ag/AgCl electrodes at points every 90° around the pore. Ca^{2+} selectivity is imparted through the ETH-5234 calcium ion-selective membrane coating. Up to sixteen spores (one per pore) can be loaded on one CEL-C chip and measurements taken simultaneously from each. The electrode and pore arrangement ensures that no electrode is further than 10 μM from the surface of the spore contained in it.

Collaboration was done with Aeraj ul Haque for set-up of the system using untreated and treated spores. Preparation and usage of the CEL-C sytem was as published (ul Haque et al., 2006). Conditioned chips were first assayed for the number of functional electrodes because the chips had been stored for a while. The test was done by examining the responsiveness of the electrodes to $CaCl_2$ standard solutions. Properly functioning electrodes exhibit a linear slope when electrode potential is plotted versus decade changes in standard concentrations. This check also served as a means of calibrating the electrodes. Due to the age of the chips, only those with more than half of the pores functioning properly were used for subsequent assays. Some pores were left unloaded as reference, but of the used pores typically 8-10 recordings of sufficient quality were obtained for further analysis.

Drugs were prepared as above and tested for direct interaction with the chip system by application to empty wells. Spore measurements were taken in DEDC (dual electrode differential coupling) mode, which measures the potential difference between

either a top-bottom or side-side electrode pair. Positive changes in DEDC mode indicate increasingly larger differences in Ca^{2+} concentrations between the top and bottom of the spore, with a greater efflux at the top (negative readings indicate the opposite). The behavior of untreated spores was reported in the paper on the CEL-C fabrication (ul Haque et al., 2006). The effects of 180° rotation on the calcium flux were also investigated. For testing of drug treatments, ½ MS containing the indicated concentration of inhibitor was applied to the spores at the indicated times after light exposure and spore set up, this exposure necessarily required that the drug penetrate the agarose overlay. One replicate of each drug exposure was run while I was at Purdue. Subsequent replicates were carried out by ul Haque using the established protocols. Data processing and graph generation was performed by ul Haque and Porterfield.

RESULTS

Drug Effects on Spore Polarity

BHQ has small but significant effects on the alignment of rhizoids. As can be seen in Figure 3.1, BHQ increases the percentage of downward growing rhizoids at 50 μM and higher concentrations. DMSO does not impact spore axis alignment and BHQ has similar results when presented in 0.1% ethanol. DMSO was chosen for the majority of experiments for consistency with other drug treatments.

Treatment with EY did not induce statistically significant alterations in polarity at any tested concentrations. Changes in rhizoid polarity were not achieved using either the water soluble disodium salt or DMSO soluble free acid forms of EY at a wide range of concentrations (0.02 μM to 10 μM). Figure 3.2 shows the effects on rhizoid emergence of spores exposed to Na_2EY at several concentrations and on different days. Co-treatment with 100 μM Na_2EY and either 50 μM or 100 μM BHQ during the first 24 hours post-

light exposure had a small, but not statistically significant, increase in downward growing rhizoid percentage over treatment with BHQ alone (Figure 3.3).

Treatment with the inhibitors impacted rhizoid growth (Table 3.1). At 100 μM BHQ, rhizoid emergence rates began to decline in a statistically significant manner and 0% of spores appear to germinate in the presence of 1000 μM BHQ. However, small prothalli will emerge by the 4th day post-light exposure even in the absence of rhizoid growth. While limited exposure to EY does not impact rhizoid growth, continuous exposure inhibits rhizoid emergence in a fashion similar to BHQ. Due to the light sensitivity of EY, continuous exposure is achieved through daily media changes. This continuous treatment of spores with 10 μM Na_2EY results in 0% rhizoid emergence, but these spores will develop small thalli. If the inhibitor is not refreshed for the 5th day a very small number (<1%) of short rhizoids will develop. This effect is independent of the form of EY since continuous application of 2 μM H_2EY results in a significant decrease in rhizoid emergence rates, though that concentration is not enough to completely block rhizoid emergence.

Drug Effects on Calcium Flux

Overall trends in the changes to the calcium flux were compared to published responses of untreated germinating spores (Figure 3.4) (ul Haque et al., 2006). None of the drugs presented here had an inherent impact on electrode readings or function. In contrast, $GdCl_3$, a treatment of potential interest, had direct dampening effects on the chip measurments, likely due to Gd^{3+} interacting negatively with the selective membrane. The $GdCl_3$ could be washed out and the chip readings would behave normally again. The calcium channel blocker nifedipine, previously shown to dramatically lower the calcium flux, results in a plateau when measured on the CEL-C biochip (Figure 3.5). Application of 100 μM nifedipine causes the spores to exhibit a flat, elevated calcium flux, though the

ratio value is about half that of a maximally responding normal spore. During the recording, the increase does not return to a ratio of 1 (zero on the log scale) as it does in the untreated germinating spores by 19 hours. Treatment with H_2EY, the SERCA inhibitor, showed a trend towards suppression of the calcium flux (Figure 3.6). Exposure to the chemical causes a nearly complete abolishment of the calcium differential between the two recording electrodes. Finally, BHQ, the PM Ca^{2+}-ATPase inhibitor, shows a response altered from normal (Figure 3.7). After application the differential continues to increase, matching untreated ratios, but after reaching a maximum it drops off prematurely (around 4.5 hours), and in a manner distinct from an untreated spore which maintains the high differential until around 12 hours.

DISCUSSION

Since there is such a large efflux of calcium from the top of the spore during the gravity fixation window, it was expected that disruption of that current through use of PM specific Ca^{2+}-ATPase inhibitors would lead to disorientation of the germinating spores. This was not found to be the case. Per the literature (Beffagna et al., 2000; Romani et al., 2004), 0.2 μM of the water soluble form of EY is sufficient to inhibit PM Ca^{2+}-ATPase activity in cell cultures and even smaller concentrations are satisfactory for PM preparations (De Michelis et al., 1993). The DMSO soluble form was limited to concentrations 2 μM and lower due to precipitation at higher levels, yet the water soluble disodium salt form did not impact polar axis alignment at 100 μM concentrations. However, continuous application of high concentrations of EY impacts a specific aspect of cell growth. Continuously exposed spores will not develop rhizoids yet will still undergo cell division and produce green prothalli. These effects are explained through inhibition of the tip growth, a process in which Ca^{2+}-ATPases have an established role

(Schiott et al., 2004). So while PM Ca^{2+}-ATPases are required for tip growth, they are not for normal polar axis development, axis alignment, cell division, or major homeostasis in *C. richardii* spores.

Based on tip-growth effects, EY is clearly capable of interaction with the spores. However, it is possible that this effect is limited to periods after the spore coat has cracked. Opening of the spore coat does not occur for 20-30 hours after polarity fixation so it is entirely possible that the spore coat may be acting as a barrier to this drug and the inability of EY to affect polarity may be simply due to the inaccessibility of the plasma membrane. To address this possibility it was necessary to examine if EY could alter the calcium flux. In collaboration with Dr. D. Marshall Porterfield and Aeraj al Haque this question was addressed by assaying the calcium current on a microchip capable of measuring relative calcium fluxes in real time. Initial tests with the system involved nifedipine. We know from the previous electrode studies that 100 μM nifedipine can dramatically reduce (~40 fold) the efflux of calcium from the top of the spore as well as the side (~15 fold less) (Chatterjee et al., 2000). This makes the results obtained with the CEL-C chip somewhat problematic since application of nifiedipine causes a plateau in the ratio measured by the electrode pair rather than indicating an elimination of the flux altogether (Figure 3.4). However, while 100 μM nifedipine is capable of causing random axis alignments it does not entirely abolish the calcium flux, it only dramatically reduces it. It is likely that the residual steady flux is a reflection of the remaining channel, and subsequently pump, activity. This ratio in the nifedipine-treated spores is about half that of a normally germinating spore and so likely represents a decreased flux, in both magnitude and ratio. Calcium extrusion rates are clearly linked to Ca^{2+}-ATPase activity (Rasi-caldogno et al., 1987; Luoni et al., 2000) and the pumps are responsive (Romani et al., 2004) in such a way that implicates a role in adjusting intracellular calcium

concentrations (Kordyum, 2003). A lower influx would be expected to induce a lower efflux, a pattern seen through the initial electrode readings and here in the decrease in the overall ratio maximum. The fact that nifedipine can impact axis alignment without completely removing the calcium flux implies that there is a threshold level to the gravity directed polarity.

Returning to the question of the effects of EY on the calcium flux, results with EY showed that application of 2 μM H_2EY could alter normal calcium flux patterns during the first 24 h after the current is initiated. The drug can therefore penetrate the cell and have an effect prior to opening of the spore coat. Further, the change in pattern of the Ca^{2+} flux is as one would expect from the inhibition of PM Ca^{2+} pumps. From the previous electrode studies we know that the topside efflux is stronger than the influx at the bottom of the spore. Therefore, blocking the efflux of the Ca^{2+} from the top of the spore would be expected to result in a dramatic decrease in the electrode differential of the CEL-C biochip, the pattern that was observed (Figure 3.6).

A role for PM Ca^{2+}-ATPases in tip growth has been established in *Arabidopsis* pollen. ACA9 localizes to pollen plasma membranes, and T-DNA insertional mutants have reduced pollen tube growth (Schiott et al., 2004). Interestingly, ACA9 falls within the subfamily of *Arabidopsis* Ca^{2+}-ATPases containing isoforms 8, 9, and 10 (Baxter et al., 2003; Schiott et al., 2004). ACA8, the isoform most similar to CrACA1 (see chapter 2), has also been localized to plasma membranes (Bonza et al., 2000). The parallel to pollen Ca^{2+}-ATPases along with the information that EY does not affect polarity but does inhibit rhizoid growth further reinforces the notion that PM Ca^{2+}-ATPases are important for tip growth, but not for the gravity-directed polarity establishment. Schiott, Romanowsky et al. (2004) speculate that the poor growth of *aca9* pollen is due to short circuiting of oscillatory Ca^{2+} waves that occur at the tip of a growing pollen tube. The

CEL-C measurements of untreated germinating spores show the overall trend of a rise and fall in the calcium differential on the time scale of hours but it hasn't been established if smaller oscillations are occurring within this overall change. A further analysis of these measurements by Fourier transformation would be a viable approach to look for such patterns, but this analysis has not yet been performed. So it remains to be seen if gravity-directed axis orientation requires the same cycling of Ca^{2+} that tip growth does.

One of the simpler models for calcium-dependent axis orientation is that an internal localization of calcium provides for or participates in the establishment of asymmetry. Calcium fluxes are predictive of rhizoid, pollen tube, and root hair outgrowths and calcium can modulate the polymerization of actin filaments. However, based on the ability of *C. richardii* spores to develop polarity in micro gravity normally (Roux et al., 2003), it is more likely that gravity calcium movements are a part of the alignment process and that the spore is inherently capable of establishing polarity. This is reminiscent of how *Fucus* zygotes align their polar development to external cues while having an initial polarity based upon sperm entry (Hable and Kropf, 2000).

A basic model depicting calcium concentrations in a germinating spore is given in Figure 3.8. Channels appear to be the keystone of the process since inhibition of calcium channels by nifedipine not only decreases polar axis alignment, but also causes a dramatic decline in the topside calcium efflux (Chatterjee et al., 2000). This also indicates that efflux is initially tied to influx. The influx of calcium in both the pressure model and statolith model is often assumed to occur via mechanosensitive channels. Additional experiments using the CEL-C biochip have shown that the magnitude of the calcium flux differential changes in synch with relative g-forces (Salmi et al., 2007), offering exciting confirmation of the mechanosensitive aspect of the calcium channels. We believe that

these channels establish a localized region of high Ca^{2+} near the bottom of the spore in conjunction with calcium pumps. Active calmodulin would stimulate PM Ca^{2+}-ATPases to clear the cytoplasm of calcium. With the rapid reversibility of the calcium flux, it is unlikely that this clearing would be localized. The influx at the bottom of the spore is most probably a net movement of calcium, with a stronger channel influx than the PM Ca^{2+}-ATPases could counteract. As expected with this, as one moves away from the bottom of the spore the efflux becomes stronger (Chatterjee et al., 2000; Stout, 2004). The large efflux from the top of the spore would be accounted for by an unopposed outward movement (i.e. active pumps and inactive channels). In this model the absence of PM Ca^{2+}-ATPase activity would not completely disrupt the system because other mechanisms, including that of endomembrane Ca^{2+}-ATPases, should be sufficient to maintain spore viability and polarity by sequestration of cytoplasmic calcium into organelles.

The enhancing effect of BHQ on spore polarity indicates that the natural activity of SERCA pumps dampens polar axis alignment. With this model, SERCA pump inhibition leads to higher cytoplasmic Ca^{2+} concentrations and subsequently a stronger response. *pmc1* mutant yeast demonstrate growth changes due to higher cytoplasmic calcium concentrations caused by calmodulin and calcineurin activation (Cunningham and Fink, 1994). The mechanisms causing growth changes in *C. richardii* spores could be occurring by two different methods. First, inhibition of endomembrane Ca^{2+}-ATPases with BHQ would result in higher local [Ca^{2+}] since the only means of calcium exit from the spore would be through the plasma membrane, which, via the longest path, could be up to 100 μM away. A gradient of calcium would still exist in this case since localized activation of channels would still result in a net efflux at the top of the spore but the total

internal [Ca^{2+}] would be greater. This could potentially allow for a stronger signal and a higher percentage of spores correctly orienting to gravity.

Another possibility is that BHQ is initiating a Ca^{2+} Release-Activated Ca^{2+} (CRAC) channel response. In animal systems these channels are relevant to non-excitatory cells. While it would generally be considered that plant cells are of the non-excitatory variety, plants are capable of the generation and propagation of action potentials (APs). The most dramatic example of this is the action potential that is involved in the movement of the leaves of the touch-responsive *Mimosa*. In relation to the spore system, APs in plants also require increased cytoplasmic Ca^{2+} levels (Fromm and Lautner, 2007). However, long distance communications are of little use to a single cell so it seems unlikely that the germinating spores of *Ceratopteris* would be utilizing action potentials in polarity establishment. Hence it is probably safest to assume that, in this case at least, they are behaving as non-excitatory cells.

CRAC channel activation in animal cells is correlated with depletion of calcium from the ER. It is theorized that Stim1, an integral ER membrane protein, interacts with CRAC channels or their associated proteins, and that upon depletion of Ca^{2+} from the ER, elements of the ER physically move to associate with the plasma membrane. This association forms co-localized puncta of Stim1 and active Ca^{2+} channels, giving at least a spatial and temporal relation to the two (Luik et al., 2006; Wu et al., 2006). This interaction of two membrane systems is quite similar to the proposed mechanism by which sedimenting plastids in *Chara* function not through pressure but by molecular interactions of associated membrane proteins (Limbach et al., 2005). Of interest to the present study is that thapsigargin, the ER-type Ca^{2+}-ATPase inhibitor functionally related to BHQ, can be used to deplete ER stores of Ca^{2+} (hence this process is also referred to as "store operated") and thus induce uptake of extracellular calcium via CRAC channels.

Rather than increasing cytoplasmic Ca^{2+} through slower sequestration, BHQ may be increasing uptake via activation of additional, non-mechanosensitive calcium channels. The requirement for specific membrane interactions also allows this activation process to be directed rather than general.

A current literature search does not produce any results regarding CRAC channels in plant systems, nor are there any obviously similar sequences to some of the animal players. Nonetheless, there is some amount of support for this idea from the results of exposing spores to BHQ and EY together. Inhibiting both endo- and plasma membrane Ca^{2+}-ATPases would theoretically have a drastic impact on general spore viability. However, when exposed to even 100 μM BHQ with 10 μM EY, the spores show no growth defects. In his review of calcium signaling of plant cells in altered gravity situations (Kordyum, 2003) discusses the regulation of Ca^{2+} as a regulatory messenger of gravity induced changes, specifically with alterations in Ca^{2+} influx/efflux. He states that "Thus, an increase of Ca^{2+} concentration in plant cells, in particular root hairs, observed in altered gravity, happened mainly due to activation of mechanosensitive calcium channels and inhibition of Ca^{2+}-ATPase activity." The effects of nifedipine along with the relative indifference of the spore growth to EY indicates that channels are the more vital of the two components considered. BHQ may be playing a dual role by not only inhibiting endomembrane Ca^{2+}-ATPase, but more importantly activating additional calcium uptake via CRAC channels caused by the secondary ER-depletion effect of a thapsigargin like inhibitor. The curve of the calcium flux supports this idea (Figure 3.7). The maximum flux ratio occurs earlier than in the untreated spores but the maximal flux is not maintained for as long. Rather, there is a steady decline in the potential difference between the electrodes which may be indicative of a decline in available calcium caused by reduced or non-replenishment of organelle stores.

Relevant to the discussion of Ca^{2+}-ATPase inhibitors in plant gravity perception and response, recent work in *Arabidopsis* roots requires comment. Urbina et al. (2006) investigated the effects of thapisgargin on root gravitropic responses. The authors found statistically significant depression of root curvature in response to gravistimulation at 0.1 and 0.5 μM thapsigargin without corresponding alterations in root growth rates. This appears to be in direct conflict with the above reported results that BHQ is capable of increasing the axis alignment of *Ceratopteris* rhizoids. The obvious difference is that we are comparing the polarity fixation of a single cell to gravitropic growth changes of an angiosperm root. I propose that the inhibition of sensitive Ca^{2+}-ATPases has the same impact on both systems but the difference in response is due to the specific cells affected.

Urbina et al. (2006) used a membrane-permeable fluorescent version of thapsigargin (BODIPY FL thapsigargin) to examine the cellular targets of thapsigargin. They found that BODIPY FL thapsigargin localized to the elongation zone and the tip but not at the quiescent center or meristematic region of the root. This does indicate that thapsigargin is most likely not affecting the primary sensors of gravity (the columella cells) while it may be inhibiting the actual effectors of gravitropism (the cells in the elongation zone). An additional feature of interest is the localization of BODIPY FL thapsigargin to the root cap. The authors suggest that since thapsigargin is a plant-derived compound it may have an endogenous function in plant cells. The inhibition of gravitropic responses by thapsigargin coupled with its localization to the root cap is suggestive of the natural touch-inhibition of gravity responses documented by Massa and Gilroy (2003). Contact of a growing root tip to a physical barrier causes a decrease in the angle of root growth. The growth angle also changes a function of the ability of various mutant plants to respond to gravity, poorer gravity responders show shallower angles of growth against the barrier.

We know that the touch stimulus is rapidly transduced into cytoplasmic calcium changes (Knight et al., 1991; Knight et al., 1992), so alterations to calcium mobility would certainly be expected to impact touch responsiveness. Further, if thapsigargin causes store operated Ca^{2+} release in the cap cells, then we should expect a response similar to when caps are touch-stimulated, which is what Urbina et al. found; thapsigargin dampens gravitropism. Since thapsigargin does not have general localization in the root system, it would be of great value to see if inhibition of SERCA pumps in columella cells has an impact on gravitropism in a manner consistent with the alterations demonstrated here in *C. richardii* spores.

As a final point of discussion, it is worth briefly commenting on the lower than expected downward growth percentages observed for the majority of experiments. The differences in treatments cannot be attributed to variations in population or media. In all cases, the population of spores used for each experiment was kept internally consistent through use of one spore collection and one tube for sterilization, dark-soaking, and sowing. A variety of different spore collections of different ages showed the same responses. Spores were only exposed to unique environments after sowing onto the monofilament mesh strips, at which point the treated liquid medium was applied. This is kept as consistent as possible by preparation of large batches of pH adjusted ½ MS medium which was then divided for additions of 1% agarose for sowing or appropriate inhibitor concentrations. Light and position effects in the growth chamber are minimized by randomly distributing the upright tubes in the holding racks at initial racking, all subsequent media changes, and at least once per 24 h. Differences in rhizoid alignment percentages could be due to exposure to slightly different conditions than previously published work, namely being submerged in media after sowing in 1% agarose (previous work used 0.5%) and the lighting conditions in the new growth cabinet I used. Regardless

of the underlying causes, the data presented here were highly repeatable and the tweaking of conditions to achieve previously published alignment rates was not worth the time investment.

SUMMARY

Our results on Ca^{2+}-ATPase inhibitor effects on *C. richardii* spore polar axis alignment and on the gravity-directed calcium current support previous work and offer new insights into early steps in gravity sensing and response. Plasma membrane Ca^{2+}-ATPases have large impacts on the calcium flux and rhizoid growth but play a relatively minor role in axis alignment. This corroborates previous work illustrating PM-type Ca^{2+}-ATPase involvement in the tip-growth of pollen tubes (Schiott et al., 2004).

The results obtained in this investigation of endomembrane-type Ca^{2+}-ATPases are novel. Our data make it clear that these transporters have major roles in both tip growth and axis alignment. While blockage of SERCA pumps inhibits rhizoid growth it actually improves the alignment of the spores' polar axis to the gravity vector. The model for gravity perception responses in *C. richardii* spores involves the initial influx of calcium into the bottom of the spore through mechanosenstive calcium channels followed by Ca^{2+} dependent activation of Ca^{2+}-ATPases. The activity of the pumps and channels in concert results in a bottom-localized calcium pool of sufficient threshold to induce fixation of the polar axis. The enhancement of axis alignment by BHQ, the alterations in the typical flux measurements by BHQ, and the lack of growth defects from BHQ and EY point to the potential for store-operated calcium movement in plant systems, a process that could enhance the localization or magnitude of the gravity-directed calcium signal. The work presented represents an increase in our knowledge of one way a single cell can respond to the force of gravity, offering testable hypotheses to further refine

pressure and membrane-membrane interaction models of gravity perception and response through incorporation of calcium localization.

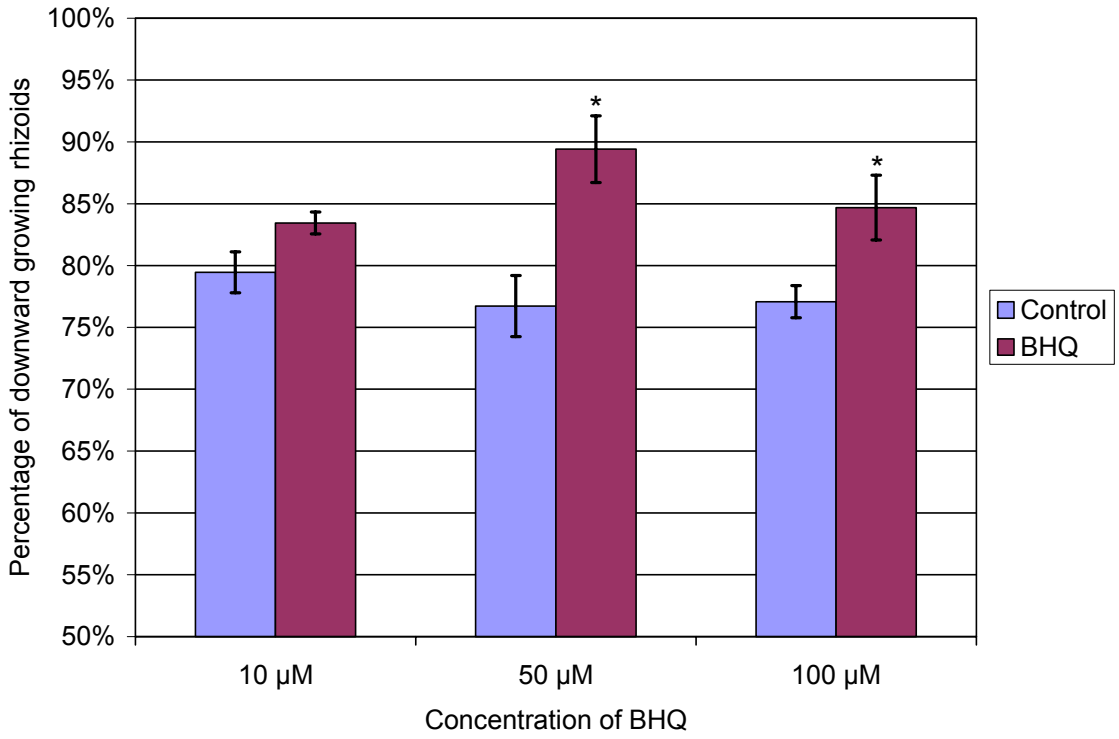

Figure 3.1: Effects of BHQ on spore polarity.

Spores were exposed to varying concentrations of BHQ from 1 to 24 hours post-light exposure. All samples had a final concentration of 0.1% (v/v) DMSO. The average percentage of downward growing rhizoids is from the spores presenting rhizoids of one spore diameter or greater. Treatments statistically different from controls, as judged by a two-sample unequal variance Student's t-Test ($p < 0.05$), are indicated with an asterisk. For both control and BHQ samples of 10 µM: $n = 9$ from a total of 680 and 518 scorable spores, respectively; 50 µM $n = 8$, 628 and 624; 100 µM $n = 8$, 686 and 370. Error bars represent standard error.

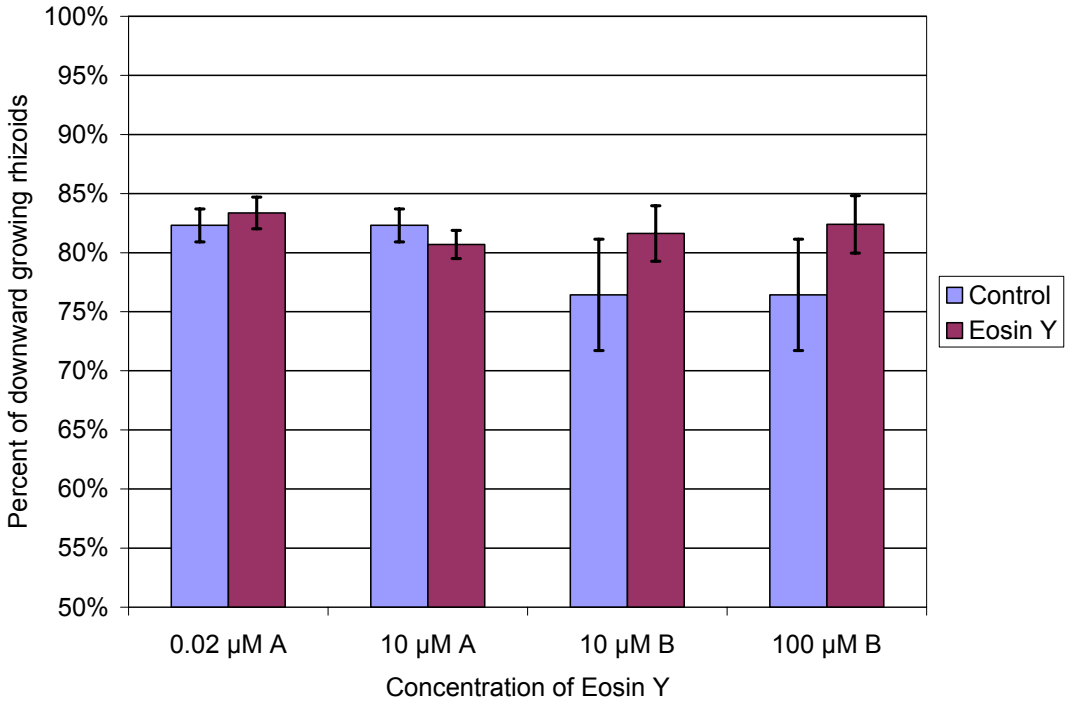

Figure 3.2: Effects of Na_2EY on spore polarity.

Spores were exposed to varying concentrations of Na_2EY from 1 to 24 hours post-light exposure. Control samples were left untreated. The average percentage of downward growing rhizoids is from those presenting rhizoids of one spore diameter or greater. The first two pairs (A) were performed on a different day than the last two pairs (B). A two-sample unequal variance Student's t-Test showed no treatments as statistically different from controls ($p > 0.4$). *n* values and total number of scoreable spores counted for each pair were as follows: 0.02 µM A $n = 5$, 368 and 366; 10 µM A $n = 5$, 368 and 464; 10 µM B $n = 8$, 194 and 239; 100 µM B $n = 8$, 194 and 121. Error bars represent standard error.

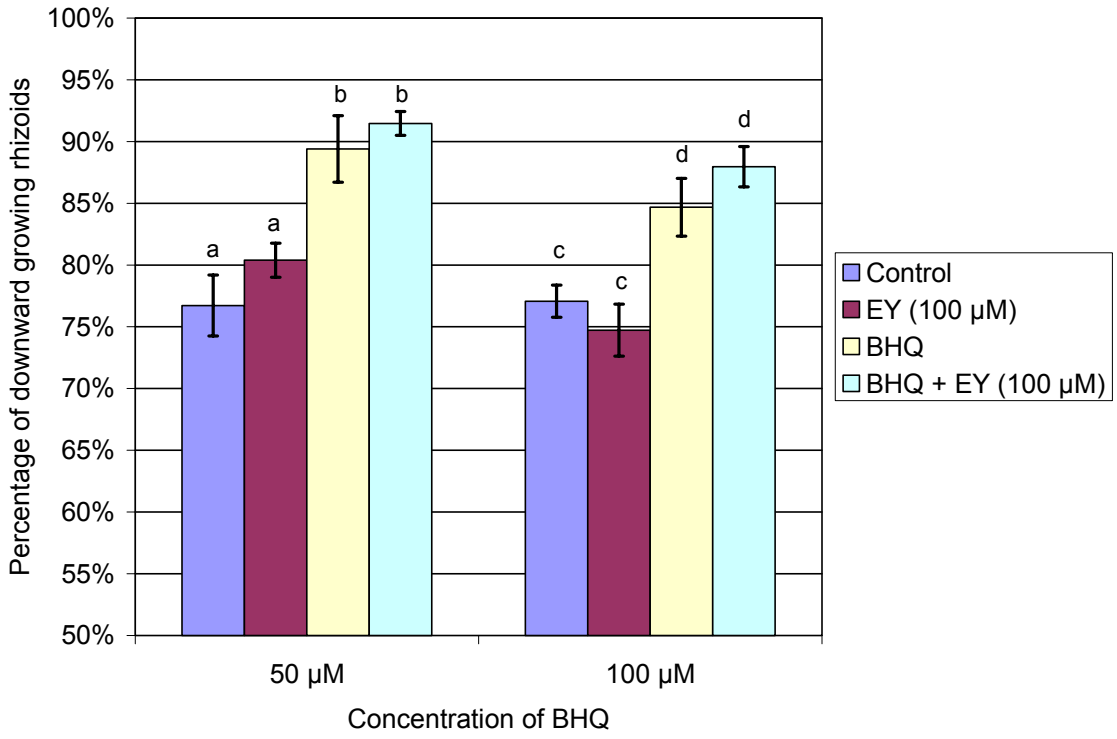

Figure 3.3: Effects of co-treament of BHQ and 100 µM Na_2EY on spore polarity.

Spores were exposed from 1 to 24 hours post-light exposure to 100 µM Na_2EY, 50 µM BHQ, 100 µM BHQ, or both Na_2EY and 50 or 100 µM BHQ. All samples had a final concentration of 0.1% DMSO (v/v). The average percentage of downward growing rhizoids is from those presenting rhizoids of one spore diameter or greater. The 50 µM BHQ exposure was performed on a different day than the 100 µM. Two-sample unequal variance Student's t-Tests were performed separately on each treatment group. Within one data set, statistically different averages ($p < 0.05$) are designated by different lower case letters. Averages with the same letter were found to not be statistically different from one another ($p > 0.2$). $n = 8$ for all conditions in the 50 µM treatment, total scorable spores counted per condition were: Control 628, EY 569, BHQ 642, BHQ + EY 586. $n = 10$ for the control condition and 8 for all others in the 100 µM treatment, total scorable spores counted for each condition were: Control 686, EY 652, BHQ 426, BHQ + EY 481. Error bars represent standard error.

Table 3.1: Effects of Ca^{2+}-ATPase inhibitors on rhizoid emergence.

Spores were exposed for 24 hours after light exposure to BHQ or continuously for 4 days to Eosin Y. Emergence percentages statistically significant from their respective controls are indicated with an asterisk ($p < 0.05$).

	Concentration of inhibitor					
	0 μM	2 μM	10 μM	30 μM	100 μM	1000 μM
BHQ	85.6%			87.0%	77.1%*	0%*
Na_2EY	70.0%		0%*			
H_2EY	74.6%	58.4%*				

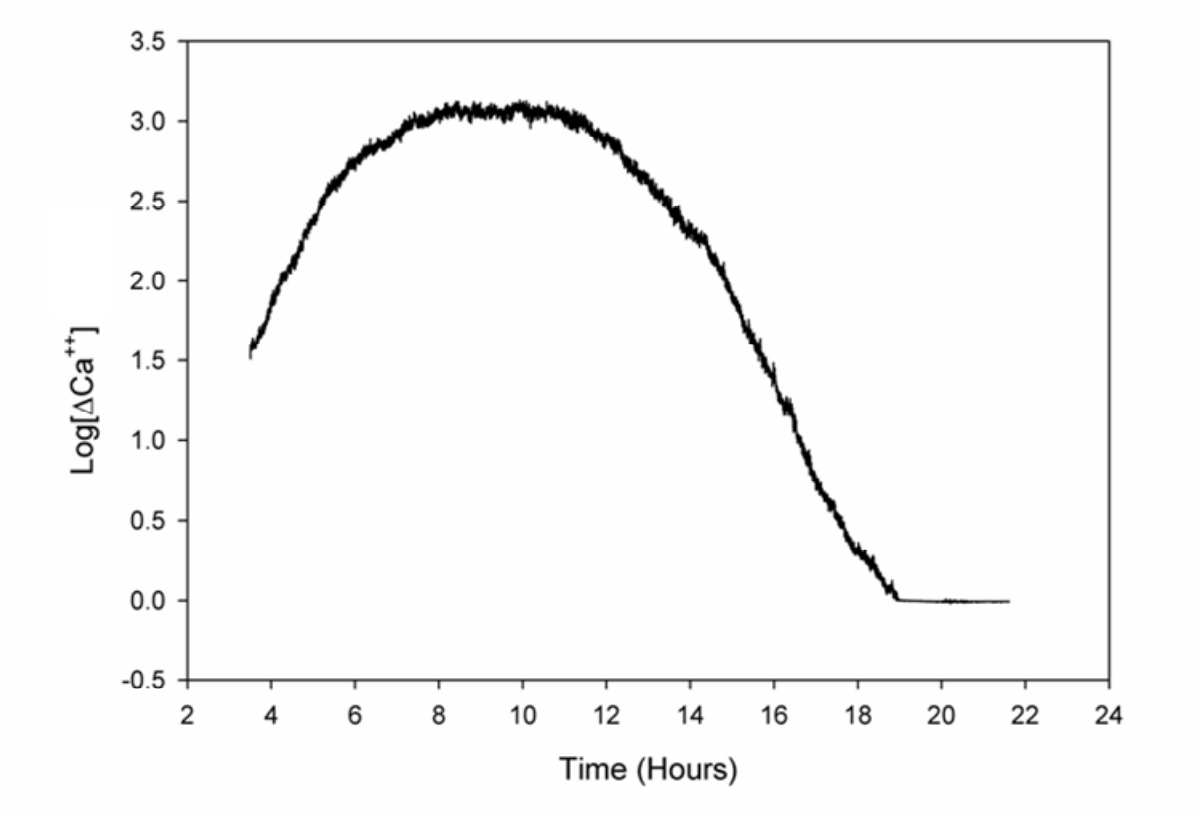

Figure 3.4: Representative data of the top-bottom calcium flux of normally germinating *C. richardii* spores.

Surface sterilized, pre-soaked spores were exposed to light and loaded onto the CEL-C biochip and immobilized with 1% agar medium. This curve is representative of ten of fourteen loaded spores exhibiting this pattern. Similar results were achieved in six additional replicates. Presented here as reference, from ul Haque, Rokkam et al. (2006)

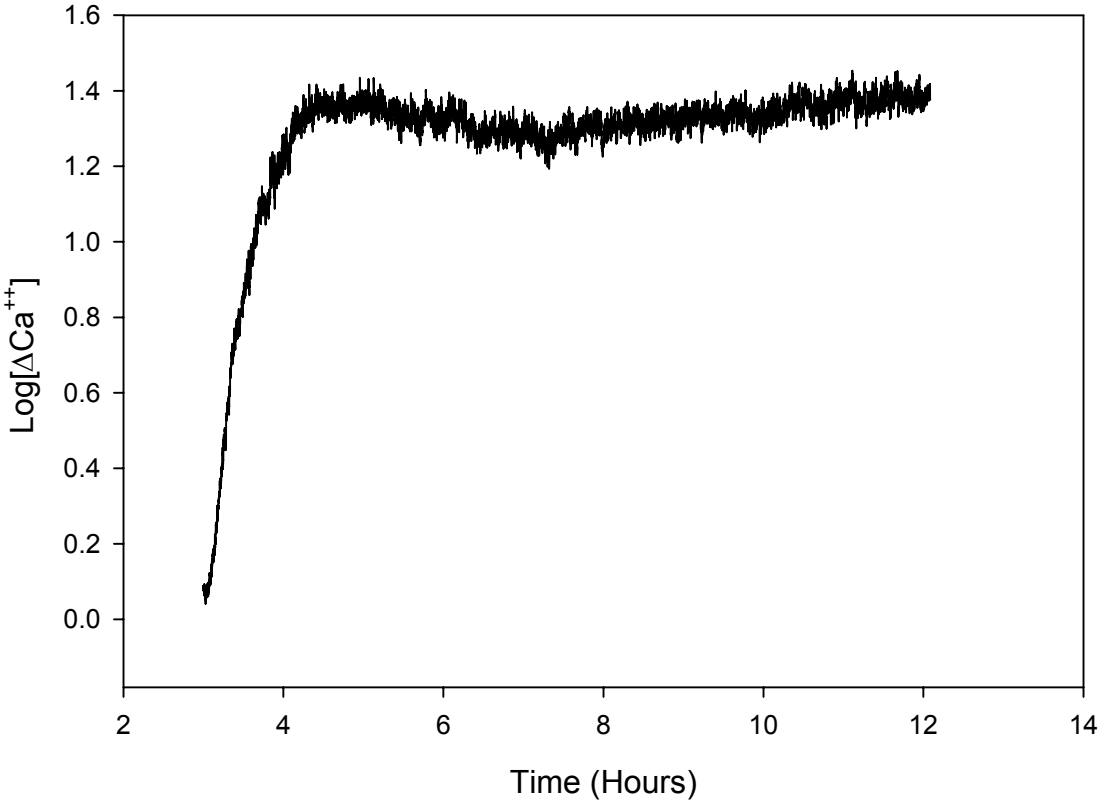

Figure 3.5: Representative effects of the calcium channel blocker nifedipine on the top-bottom calcium flux of *C. richardii* spores.

Surface sterilized, pre-soaked spores were exposed to light and loaded onto the CEL-C biochip and immobilized with 1% agar medium. The top-bottom electrode pair was measured continuously in DEDC mode for the indicated time. Nifedipine was added to the spores at 4 hours. This curve is representative of seven of ten loaded spores exhibiting this pattern. Similar results were achieved in two additional replicates.

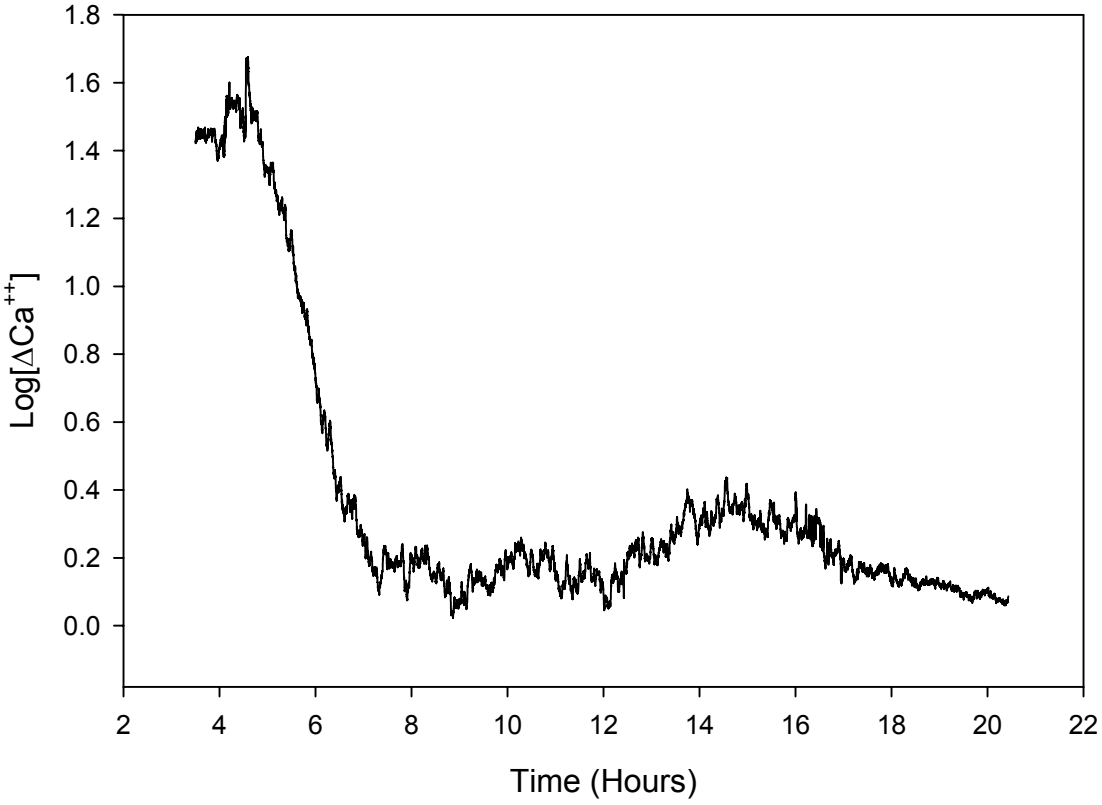

Figure 3.6: Representative effects of the calcium pump blocker eosin Y on the top-bottom calcium flux of *C. richardii* spores.

Surface sterilized, pre-soaked spores were exposed to light and loaded onto the CEL-C biochip and immobilized with 1% agar medium. The top-bottom electrode pair was measured continuously in DEDC mode for the indicated time. Eosin Y was added to the spores at 5 hours. This curve is representative of five of eight loaded spores exhibiting this pattern. Similar results were achieved in two additional replicates.

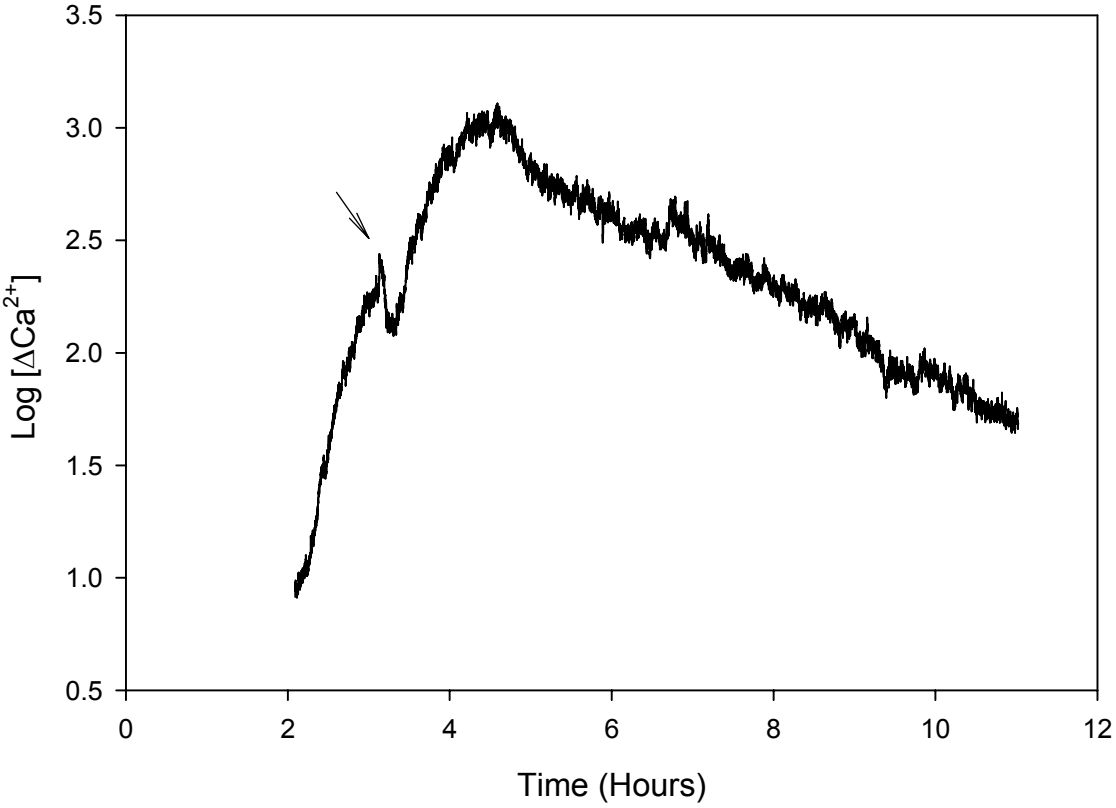

Figure 3.7: Representative effects of the calcium pump blocker BHQ on the top-bottom calcium flux of *C. richardii* spores.

Surface sterilized, pre-soaked spores were exposed to light and loaded onto the CEL-C biochip and immobilized with 1% agar medium. The top-bottom electrode pair was measured continuously in DEDC mode for the indicated time. BHQ was added to the spores at 3 hours (arrow). This curve is representative of the responding spores on the biochip. Similar results were achieved in replicate.

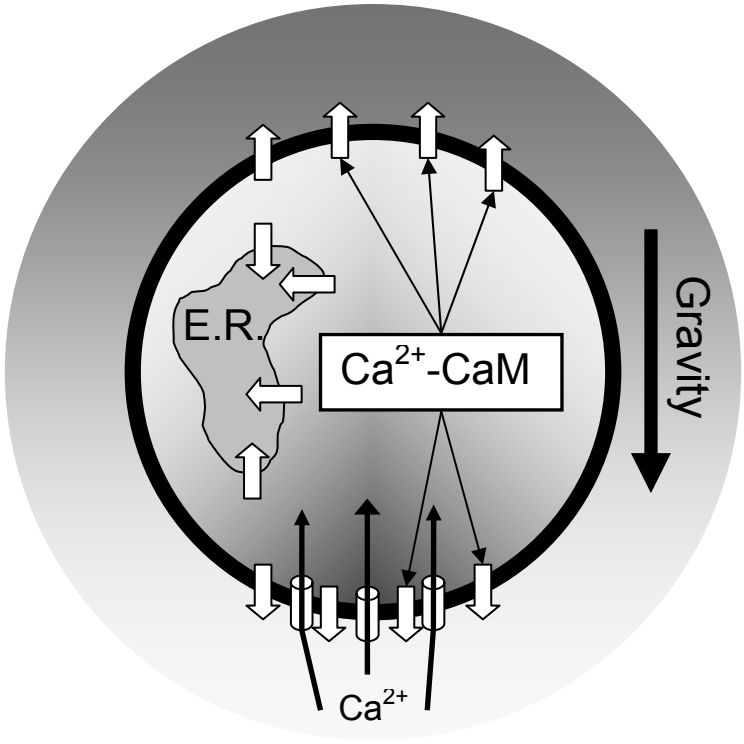

Figure 3.8: Model for Ca^{2+} localization in germinating spores via Ca^{2+}-ATPase and channel activity.

Ca^{2+} and both its cytoplasmic and external concentration are represented by shades of grey (darker being more concentrated). Movement of calcium, molecular interaction, and the gravity vector are represented by the thin solid arrows. Cylinders in the large black circle of the plasma membrane represent calcium channels while the white block arrows are Ca^{2+}-ATPases. Both of these components are theorized to be localized over the entirety of the PM but the locations of importance are at the top and bottom of the spore. We believe that the gravity-directed polar axis alignment is established in part through concentration of Ca^{2+} at the bottom of the spore. An inward directed calcium current is mediated by calcium channels whereby activated calmodulin (Ca^{2+}-CaM) stimulates the PM Ca^{2+}-ATPases to efflux. The net efflux movement of calcium at the top of the spore is greater than the bottom due to the un-opposed action of the Ca^{2+}-ATPase at that location. The endoplasmic reticulum (E.R.) is also likely to play a role either through clearing of the cytoplasm of Ca^{2+} or through its potential involvement in store operated calcium release. The summary effect of these channel and pump components is an externally measurable Ca^{2+} influx at the bottom of the spore and an efflux from the top. Internally, a concentration of Ca^{2+} is maintained at the bottom of the spore through the channel influx while the rest of the cytoplasm is continually cleared via both ER and PM Ca^{2+}-ATPases

CHAPTER 4: CONCLUSION

Germinating *C. richardii* spores have a fast-responding, gravity-directed calcium current with a limited period of responsiveness, making them an ideal system for the study of how the gravity vector can be interpreted by single cells. Because this current involves the strong efflux of Ca^{2+} ions, it was theorized that calcium pumps would play a key role in the process and, by extrapolation, the alignment of a polar axis. To test this role, a Ca^{2+}-ATPase was cloned and characterized from *Ceratopteris* and Ca^{2+}-ATPase inhibitors were used to dissect the part that Ca^{2+}-ATPases play in the efflux and polar axis alignment.

The first cloned Ca^{2+}-ATPase from *Ceratopteris*, designated CrACA1, was found to have remarkable similarity to plasma membrane localized Ca^{2+}-ATPases from the distantly related *Arabidopsis thaliana*. The RNA and protein profiles of CrACA1 indicate that this Ca^{2+}-ATPase is present during the period of maximal calcium flux making it a possible participant in this gravity-directed process. Due to the limitations of the *Ceratopteris* system, it was not feasible to directly connect CrACA1 to the calcium efflux through genetic manipulations. However, a number of characterized Ca^{2+}-ATPase inhibitors allowed us to examine how general classes (plasma membrane versus endo-membrane) of Ca^{2+}-ATPase can both contribute to the calcium efflux and the alignment of the spores' polar axis to the gravity vector.

Using the newly developed CEL-C biochip, in conjunction with the Ca^{2+}-ATPase inhibitors Eosin Y and BHQ, it was found that Ca^{2+}-ATPases are integral to the germination process of the spores, but not in the way anticipated. Since the efflux of calcium from the top of the spore was so much stronger than influx at the bottom, it was expected that the efflux components (i.e. PM-type Ca^{2+}-ATPases) would be the lynchpin. However, while EY dramatically dampened the calcium differential, it did not have any

subsequent measurable impacts on the ability of the spores to properly orient their growth to the gravity vector. Instead, the endo-membrane Ca^{2+}-ATPase inhibitor BHQ altered spore alignment by actually increasing the percentage of properly oriented rhizoids. BHQ alters the calcium efflux too, but in a manner that does not diminish the calcium differential. So the major component of the calcium efflux was actually found to have no effect on the ability of the spores to orient properly to the gravity vector while an internal component of calcium balance appears to work naturally against the correct alignment, although not to large effect.

In addition to the alignment effects of the Ca^{2+}-ATPase inhibitors, both were found to impact rhizoid emergence but not cell division. This effect fits with known functions of calcium and Ca^{2+}-ATPases in the tip growth process. The rhizoids of *Ceratopteris* undergo tip growth in a manner that is quite similar to many different cell types. The details of calcium signaling, nitric oxide signaling, and gene expression in tip growth (Bushart and Roux, 2007) play to the commonality of basic cellular processes. Gravity perception is one such basic process that may have different end points, but it would be surprising if it did not have a common underlying process for detection and initial responses.

Based on the data presented in this dissertation, it is clear that calcium is important to the gravity-directed processes of a single cell. Specifically, channel-mediated alterations of cytoplasmic calcium concentrations are the main component of early gravity-directed responses. Ca^{2+}-ATPases, and likely other modulators of calcium, play a role in both homeostasis and fine tuning of the calcium signal. It would be valuable to look for this same process occurring at a cellular level in other model systems of gravity perception and response in order to elucidate both the basic and unique aspects

of this process. As well, other model systems offer the tools for genetic manipulations for further clarifications.

In addition to gravity-related processes, it would also be of value to investigate the possibility of store-operated calcium responses in plants as well. While the specifics of the process are becoming clear in animal systems, its presence in plant systems is not entirely evident. The enhancing effects of the thapsigargin-like inhibitor BHQ raise the possibility for store-operated functionality in our plant system. As well, the membrane associations that occur during the activation of CRAC channels in animal systems are an exciting analog for how gravity perception involving plastid sedimentation could be occurring. A great benefit of studies in non-traditional model systems, as illustrated by my dissertation findings, is the generation of bridging data that can help to sort out common processes from species-specific innovations.

References

Adams-Phillips L, Barry C, Kannan P, Leclercq J, Bouzayen M, Giovannoni J (2004) Evidence that CTR1-mediated ethylene signal transduction in tomato is encoded by a multigene family whose members display distinct regulatory features. Plant Molecular Biology **54:** 387-404

Antoine AF, Faure JE, Cordeiro S, Dumas C, Rougier M, Feijo JA (2000) A calcium influx is triggered and propagates in the zygote as a wavefront during in vitro fertilization of flowering plants. Proceedings of the National Academy of Sciences of the United States of America **97:** 10643-10648

Applied Biosystems (2004) Guide to performing relative quantitiation of gene expression using real-time quantitative PCR. *In* Application Tutorial, Vol 4371095A, p 60

Baxter I, Tchieu J, Sussman MR, Boutry M, Palmgren MG, Gribskov M, Harper JF, Axelsen KB (2003) Genomic comparison of P-type ATPase ion pumps in Arabidopsis and rice. Plant Physiology **132:** 618-628

Bednarska E (1989) The effect of exogenous Ca^{2+} ions on pollen grain germination and pollen tube growth: investigations with $^{45}Ca^{2+}$ together with verapamil, La^{3+} and ruthenium red. Sexual Plant Reproduction **2:** 53-58

Beffagna N, Romani G, Sforza MC (2000) H+ fluxes at plasmalemma level: In vivo evidence for a significant contribution of the Ca2+-ATPase and for the involvement of its activity in the abscisic acid-induced changes in Egeria densa leaves. Plant Biology **2:** 168-175

Berger F, Brownlee C (1993) Ratio confocal imaging of free cytoplasmic calcium in polarizing and polarized *Fucus* zygotes. Plant Physiology **99:** 864-871

Blancaflor EB, Fasano JM, Gilroy S (1998) Mapping the functional roles of cap cells in the response of Arabidopsis primary roots to gravity. Plant Physiology **116:** 213-222

Bonza MC, Morandini P, Luoni L, Geisler M, Palmgren MG, De Michelis MI (2000) At-ACA8 encodes a plasma membrane-localized calcium-ATPase of Arabidopsis with a calmodulin-binding domain at the N terminus. Plant Physiology **123:** 1495-1505

Braun M (2002) Gravity perception requires statoliths settled on specific plasma membrane areas in characean rhizoids and protonemata. Protoplasma **219:** 150-159

Brownlee C, Pulsford AL (1988) Visualization of the Cytoplasmic Ca-2+ Gradient in Fucus-Serratus Rhizoids - Correlation with Cell Ultrastructure and Polarity. Journal of Cell Science **91:** 249-256

Bushart TJ, Roux SJ (2007) Conserved features of germination and polarized cell growth: A few insights from a pollen-fern spore comparison. Annals of Botany **99:** 9-17

Cantero A, Barthakur S, Bushart TJ, Chou S, Morgan RO, Fernandez MP, Clark GB, Roux SJ (2006) Expression profiling of the Arabidopsis annexin gene family during germination, de-etiolation and abiotic stress. Plant Physiology and Biochemistry **44:** 13-24

Charrier B, Champion A, Henry Y, Kreis M (2002) Expression profiling of the whole Arabidopsis Shaggy-like kinase multigene family by real-time reverse transcriptase-polymerase chain reaction. Plant Physiology **130:** 577-590

Chatterjee A, Porterfield DM, Smith PS, Roux SJ (2000) Gravity-directed calcium current in germinating spores of Ceratopteris richardii. Planta **210:** 607-610

Chung WS, Lee SH, Kim JC, Heo WD, Kim MC, Park CY, Park HC, Lim CO, Kim WB, Harper JF, Cho MJ (2000) Identification of a calmodulin-regulated soybean Ca2+-ATPase (SCA1) that is located in the plasma membrane. Plant Cell **12:** 1393-1407

Cove DJ (2000) The generation and modification of cell polarity. Journal of Experimental Botany **51:** 831-838

Cunningham KW, Fink GR (1994) Calcineurin-Dependent Growth-Control in Saccharomyces-Cerevisiae Mutants Lacking Pmc1, a Homolog of Plasma-Membrane Ca2+ Atpases. Journal of Cell Biology **124:** 351-363

Czechowski T, Stitt M, Altmann T, Udvardi MK, Scheible WR (2005) Genome-wide identification and testing of superior reference genes for transcript normalization in Arabidopsis. Plant Physiology **139:** 5-17

De Michelis MI, Carnelli A, Rasi-Caldogno F (1993) The Ca-2+ Pump of the Plasma-Membrane of Arabidopsis-Thaliana - Characteristics and Sensitivity to Fluorescein Derivatives. Botanica Acta **106:** 20-25

Dutta R, Robinson KR (2004) Identification and characterization of stretch-activated ion channels in pollen protoplasts. Plant Physiology **135:** 1398-1406

Edwards ES, Roux SJ (1994) Limited Period of Graviresponsiveness in Germinating Spores of Ceratopteris-Richardii. Planta **195:** 150-152

Edwards ES, Roux SJ (1998) Gravity and light control of the developmental polarity of regenerating protoplasts isolated from prothallial cells of the fern Ceratopteris richardii. Plant Cell Reports **17:** 711-716

Edwards ES, Roux SJ (1998) Influence of gravity and light on the developmental polarity of Ceratopteris richardii fern spores. Planta **205:** 553-560

Elble R (1992) A Simple and Efficient Procedure for Transformation of Yeasts. Biotechniques **13:** 18-20

Evans DE, Williams LE (1998) P-type calcium ATPases in higher plants - biochemical, molecular and functional properties. Biochimica Et Biophysica Acta-Reviews on Biomembranes **1376:** 1-25

Franklin-Tong VE, Holdaway-Clarke TL, Straatman KR, Kunke JG, Hepler PK (2002) Involvement of extracellular calcium influx in the self-incompatibility response of Papaver rhoeas. Plant Journal **29:** 333-345

Fromm J, Lautner S (2007) Electrical signals and their physiological significance in plants. Plant Cell and Environment **30:** 249-257

Gachon C, Mingam A, Charrier B (2004) Real-time PCR: what relevance to plant studies? Journal of Experimental Botany **55:** 1445-1454

Gaxiola RA, Fink GR, Hirschi KD (2002) Genetic manipulation of vacuolar proton pumps and transporters. Plant Physiology **129:** 967-973

Geisler M, Axelsen KB, Harper JF, Palmgren MG (2000) Molecular aspects of higher plant P-type Ca2+-ATPases. Biochimica Et Biophysica Acta-Biomembranes **1465:** 52-78

Golovkin M, Reddy ASN (2003) A calmodulin-binding protein from Arabidopsis has an essential role in pollen germination. Proceedings of the National Academy of Sciences of the United States of America **100:** 10558-10563

Hable WE, Kropf DL (2000) Sperm entry induces polarity in fucoid zygotes. Development **127:** 493-501

Hader DP, Hemmersbach R (1997) Graviperception and graviorientation in flagellates. Planta **203:** S7-S10

Harper JF, Hong BM, Hwang ID, Guo HQ, Stoddard R, Huang JF, Palmgren MG, Sze H (1998) A novel calmodulin-regulated Ca2+-ATPase (ACA2) from Arabidopsis with an N-terminal autoinhibitory domain. Journal of Biological Chemistry **273:** 1099-1106

Hirschi K (2001) Vacuolar H+/Ca2+ transport: who's directing the traffic? Trends in Plant Science **6:** 100-104

Holdaway-Clarke TL, Hepler PK (2003) Control of pollen tube growth: role of ion gradients and fluxes. New Phytologist **159:** 539-563

Horton P, Park K-J, Obayashi T, Nakai K (2006) Protein Subcellular Localization Prediction with WoLF PSORT. Proceedings of the 4th Annual Asia Pacific Bioinformatics Conference **APBC06:** 39-48

Jang JY, Kim DG, Kim YO, Kim JS, Kang HS (2004) An expression analysis of a gene family encoding plasma membrane aquaporins in response to abiotic stresses in Arabidopsis thaliana. Plant Molecular Biology **54:** 713-725

Khan YM, Wictome M, East JM, Lee AG (1995) Interactions of Dihydroxybenzenes with the Ca2+-Atpase - Separate Binding-Sites for Dihydroxybenzenes and Sesquiterpene. Biochemistry **34:** 14385-14393

Kiss JZ, Guisinger MM, Miller AJ, Stackhouse KS (1997) Reduced gravitropism in hypocotyls of starch-deficient mutants of Arabidopsis. Plant and Cell Physiology **38:** 518-525

Kiss JZ, Wright JB, Caspar T (1996) Gravitropism in roots of intermediate-starch mutants of Arabidopsis. Physiologia Plantarum **97:** 237-244

Knight MR, Campbell AK, Smith SM, Trewavas AJ (1991) Transgenic Plant Aequorin Reports the Effects of Touch and Cold-Shock and Elicitors on Cytoplasmic Calcium. Nature **352:** 524-526

Knight MR, Smith SM, Trewavas AJ (1992) Wind-Induced Plant Motion Immediately Increases Cytosolic Calcium. Proceedings of the National Academy of Sciences of the United States of America **89:** 4967-4971

Kordyum EL (2003) Calcium signaling in plant cells in altered gravity. *In* Space Life Sciences: Gravitational Biology: 2002, Vol 32, pp 1621-1630

Kuznetsov OA, Hasenstein KH (1996) Intracellular magnetophoresis of amyloplasts and induction of root curvature. Planta **198:** 87-94

Kuznetsov OA, Schwuchow J, Sack FD, Hasenstein KH (1999) Curvature induced by amyloplast magnetophoresis in protonemata of the moss Ceratodon purpureus. Plant Physiology **119:** 645-650

Labarga A, Pilai S, Valentin F, Anderson M, Lopez R (2005) Web services at the EBI. EMBnet.news **11:** 18-23

Limbach C, Hauslage J, Schafer C, Braun M (2005) How to activate a plant gravireceptor. Early mechanisms of gravity sensing studied in characean rhizoids during parabolic flights. Plant Physiology **139:** 1030-1040

Luik RM, Wu MM, Buchanan J, Lewis RS (2006) The elementary unit of store-operated Ca2+ entry: local activation of CRAC channels by STIM1 at ER-plasma membrane junctions. Journal of Cell Biology **174:** 815-825

Luoni L, Bonza MC, De Michelis MI (2000) H+/Ca2+ exchange driven by the plasma membrane Ca2+-ATPase of Arabidopsis thaliana reconstituted in proteoliposomes after calmodulin-affinity purification. Febs Letters **482:** 225-230

MacCleery SA, Kiss JZ (1999) Plastid sedimentation kinetics in roots of wild-type and starch-deficient mutants of Arabidopsis. Plant Physiology **120:** 183-192

Malho R, Read ND, Pais MS, Trewavas AJ (1994) Role of Cytosolic-Free Calcium in the Reorientation of Pollen-Tube Growth. Plant Journal **5:** 331-341

Massa GD, Gilroy S (2003) Touch modulates gravity sensing to regulate the growth of primary roots of Arabidopsis thaliana. Plant Journal **33:** 435-445

Moller JV, Juul B, leMaire M (1996) Structural organization, ion transport, and energy transduction of P-type ATPases. Biochimica Et Biophysica Acta-Reviews on Biomembranes **1286:** 1-51

Perrin RM, Young LS, Murthy N, Harrison BR, Wang Y, Will JL, Masson PH (2005) Gravity signal transduction in primary roots. Annals of Botany **96:** 737-743

Pfaffl MW, Horgan GW, Dempfle L (2002) Relative expression software tool (REST (c)) for group-wise comparison and statistical analysis of relative expression results in real-time PCR. Nucleic Acids Research **30**

Pillai S, Silventoinen V, Kallio K, Senger M, Sobhany S, Tate J, Velankar S, Golovin A, Henrick K, Rice P, Stoehr P, Lopez R (2005) SOAP-based services provided by the European Bioinformatics Institute. *In*, Vol 33, pp W25-28

Pittman JK, Shigaki T, Hirschi KD (2005) Evidence of differential pH regulation of the Arabidopsis vacuolar Ca2+/H+ antiporters CAX1 and CAX2. Febs Letters **579:** 2648-2656

Pu R, Robinson KR (1998) Cytoplasmic calcium gradients and calmodulin in the early development of the fucoid alga *Pelvetia compressa*. Journal of Cell Science **111:** 3197-3207

Rasi-Caldogno F, Carnelli A, Demichelis MI (1995) Identification of the Plasma-Membrane Ca2+-Atpase and of Its Autoinhibitory Domain. Plant Physiology **108:** 105-113

Rasi-caldogno F, Pugliarello MC, Demichelis MI (1987) The Ca-2+-Transport Atpase of Plant Plasma-Membrane Catalyzes a Nh+/Ca-2+ Exchange. Plant Physiology **83:** 994-1000

Romani G, Bonza MC, Filippini I, Cerana M, Beffagna N, De Michelis MI (2004) Involvement of the plasma membrane Ca2+-ATPase in the short-term response of Arabidopsis thaliana cultured cells to oligogalacturonides. Plant Biology **6:** 192-200

Roux SJ, Chatterjee A, Hillier S, Cannon T (2003) Early development of fern gametophytes in microgravity. Space Life Sciences: Missions to Mars, Radiation Biology, and Plants as a Foundation for Long-Term Life Support Systems in Space **31:** 215-220

Rutherford G, Tanurdzic M, Hasebe M, Banks J (2004) A systemic gene silencing method suitable for high throughput, reverse genetic analyses of gene function in fern gametophytes. **4:** 6

Salmi ML, Bushart TJ, Clark GB (2006) Three different mothods of expression profile and analysis in plants. Plant Tissue Culture and Biotechnology **16:** 63-73

Salmi ML, Bushart TJ, Stout SC, Roux SJ (2005) Profile and analysis of gene expression changes during early development in germinating spores of Ceratopteris richardii. Plant Physiology **138:** 1734-1745

Salmi ML, ul Haque A, Stout SC, Roux SJ, Marshall D (2007) Changes in gravity rapidly alter the magnitude and direction of a calcium current in a single cell. The University of Texas at Austin, Austin, TX

Schiott M, Romanowsky SM, Baekgaard L, Jakobsen MK, Palmgren MG, Harper JF (2004) A plant plasma membrane Ca2+ pump is required for normal pollen tube growth and fertilization. Proceedings of the National Academy of Sciences of the United States of America **101:** 9502-9507

Schwuchow JM, Kern VD, Sack FD (2002) Tip-growing cells of the moss Ceratodon purpureus are gravitropic in high-density media. Plant Physiology **130:** 2095-2100

Staves MP, Wayne R, Leopold AC (1992) Hydrostatic pressure mimics graviational pressure in characean cells. Protoplasma **168:** 141-152

Staves MP, Wayne R, Leopold AC (1997) The effect of the external medium on the gravitropic curvature of rice (Oryza sativa, Poaceae) roots. American Journal of Botany **84:** 1522-1529

Staves MP, Wayne R, Leopold AC (1997) The effect of the external medium on the gravity-induced polarity of cytoplasmic streaming in Chara corallina (Characeae). American Journal of Botany **84:** 1516-1521

Stout SC (2004) Physiological and Bioinformatic Studies on Polarity Development in *Ceratopteris richardii* spores. Dissertation. The University of Texas at Austin, Austin

Stout SC, Porterfield DM, Roux SJ (2003) Calcium signaling during polarity development in *Ceratopteris richardii*. Gravitational and Space Biology Bulletin **17:** 18

Tan BC, Joseph LM, Deng WT, Liu LJ, Li QB, Cline K, McCarty DR (2003) Molecular characterization of the Arabidopsis 9-cis epoxycarotenoid dioxygenase gene family. Plant Journal **35:** 44-56

ul Haque A, Rokkam M, De Carlo AR, Wereley ST, Roux SJ, Irazoqui PP, Porterfield DM (2006) A MEMS fabricated cell electrophysiology biochip for *in silico* calcium measurements. Sensors and Actuators B **doi:10.1016/j.snb.2006.08.043**

ul Haque A, Rokkam M, De Carlo AR, Wereley ST, Wells HW, McLamb WT, Roux SJ, Irazoqui PP, Porterfield DM (2006) Design, Fabrication and Characterization of an In Silico Cell Physiology lab for Bio Sensing Applications. Journal of Physics: Conference Series **34:** 740-746

Urbina DC, Silva H, Meisel LA (2006) The Ca2+ pump inhibitor, thapsigargin, inhibits root gravitropism in Arabidopsis thaliana. Biological Research **39:** 289-296

Wang YF, Fan LM, Zhang WZ, Zhang W, Wu WH (2004) Ca2+-permeable channels in the plasma membrane of arabidopsis pollen are regulated by actin microfilaments. Plant Physiology **136:** 3892-3904

Wayne R, Staves MP, Leopold AC (1992) The Contribution of the Extracellular-Matrix to Gravisensing in Characean Cells. Journal of Cell Science **101:** 611-623

Weisenseel MH, Nuccitelli R, Jaffe LF (1975) Large electrical currents traverse growing pollen tubes. Journal of Cell Biology **66:** 556-567

Wu MM, Buchanan J, Luik RM, Lewis RS (2006) Ca2+ store depletion causes STIM1 to accumulate in ER regions closely associated with the plasma membrane. Journal of Cell Biology **174:** 803-813

Wymer CL, Bibikova TN, Gilroy S (1997) Cytoplasmic free calcium distributions during the development of root hairs of Arabidopsis thaliana. Plant Journal **12:** 427-439

Yoder TI, Zheng HQ, Todd P, Staehelin LA (2001) Amyloplast sedimentation dynamics in maize columella cells support a new model for the gravity-sensing apparatus of roots. Plant Physiology **125:** 1045-1060

Yokoyama R, Nishitani K (2001) A comprehensive expression analysis of all members of a gene family encoding cell-wall enzymes allowed us to predict cis-regulatory regions involved in cell-wall construction in specific organs of arabidopsis. Plant and Cell Physiology **42:** 1025-1033

Yokoyama R, Rose JKC, Nishitani K (2004) A surprising diversity and abundance of xyloglucan endotransglucosylase/hydrolases in rice. Classification and expression analysis. Plant Physiology **134:** 1088-1099

Vita

Thomas James Bushart was born on July 24th, 1977 in Amherst, NY. He is the son of Darwin Robert Bushart and Luanne Bonnie Bushart. He graduated from the Jordan-Elbridge Jr.-Sr. High School in 1995 and received a B.S. in biology from the University of Rochester, Rochester, NY in 1999.

Permanent address: 1205B Inland Grn, Austin, TX 78758

This dissertation was typed by the author.